Spherical particle in Poiseuille flow between planar walls

R. B. Jones[a)]
Department of Physics, Queen Mary, University of London, London E1 4NS, United Kingdom

(Received 22 January 2004; accepted 18 March 2004)

We study a spherical mesoparticle suspended in Newtonian fluid between plane-parallel walls with incident Poiseuille flow. Using a two-dimensional Fourier transform technique we obtain a symmetric analytic expression for the Green tensor for the Stokes equations describing the creeping flow in this geometry. From the matrix elements of the Green tensor with respect to a complete vector harmonic basis, we obtain the friction matrix for the sphere. The calculation of matrix elements of the Green tensor is done in large part analytically, reducing the evaluation of these elements to a one-dimensional numerical integration. The grand resistance and mobility matrices in Cartesian form are given in terms of 13 scalar friction and mobility functions which are expressed in terms of certain matrix elements calculated in the spherical basis. Numerical calculation of these functions is shown to converge well and to agree with earlier numerical calculations based on boundary collocation. For a channel width broad with respect to the particle radius, we show that an approximation defined by a superposition of single-wall functions is reasonably accurate, but that it has large errors for a narrow channel. In the two-wall geometry the friction and mobility functions describing translation–rotation coupling change sign as a function of position between the two walls. By Stokesian dynamics calculations for a polar particle subject to a torque arising from an external field, we show that the translation–rotation coupling induces sideways migration at right angles to the direction of fluid flow. © *2004 American Institute of Physics.*
[DOI: 10.1063/1.1738637]

I. INTRODUCTION

Hydrodynamic forces play a significant role in determining the transport properties of colloidal suspensions.[1,2] In semidilute or dense macroscopic suspensions of particles with short-range or hard-sphere two-body forces, particle–particle hydrodynamic interactions are essential in determining the translational and rotational self-diffusion coefficients[3] and effective viscosity of the suspension.[4] In addition to these particle–particle effects, hydrodynamic forces between particles and the surrounding boundary can exert a strong influence on processes like sedimentation.[5] Experiments utilizing evanescent light scattering, video microscopy, and optical tweezers enable one now to measure directly the hydrodynamic interaction between one particle and a single wall,[6] between one particle and two parallel containing walls,[7,8] and even between two particles in the presence of plane walls.[9] Studies of magnetic particles in a thin fluid layer between parallel glass plates[10] and of paramagnetic particles at a water–air interface[11] have revealed microscopic properties of two-dimensional fluids and crystals. In addition recent flow experiments through an array of optical traps in a thin fluid layer between parallel walls offers the prospect of microfluidic particle sorting.[12] Because of these recent experimental advances, there is need for a better quantitative understanding of hydrodynamic interaction forces between particles and surrounding walls.

For the case of particles suspended near a single planar bounding wall, there is now a convenient representation of the friction and mobility functions for a single particle in creeping flow[13,14] and these methods can be readily extended to treat many-body hydrodynamic interactions in the presence of a single wall.[15] For particles suspended between close parallel planar walls (a common experimental situation), it is desirable to extend this treatment to encompass both the single-particle and many-particle interactions. An early approximate treatment of this problem of one particle between two walls by the method of low-order reflections was due to Ho and Leal,[16] but the first accurate calculation of the forces and torques on a single particle in shear or Poiseuille flow between parallel walls was due to Ganetos, Weinbaum, and Pfeffer[17,18] who used a numerical boundary collocation technique. They published results for a sample of different geometries. More recently, the method of reflections has been used to high order for the two-wall problem[7,19] which builds on previous solutions for the one-wall case. The drawback of the reflection technique is that, unlike the one-wall case where each force multipole has only a finite number of image multipoles, an infinite sum of multipole images is required for two walls. However, there is an alternative way to tackle the two-wall geometry. As shown earlier for one wall, the calculation of friction and mobility functions depends fundamentally on calculating certain matrix elements of the exact Green tensor for the creeping-motion Stokes equations in the given geometry.[13,15] The image method as applied to one wall is merely a means to calculate these matrix elements. For two parallel planar walls it is possible to express the Green tensor as a two-dimensional Fourier transform in such a way as to make possible the explicit calculation of all Green tensor matrix elements. This calculation is essentially

a)Fax: +44 (0)20 8981 9465. Electronic mail: r.b.jones@qmul.ac.uk

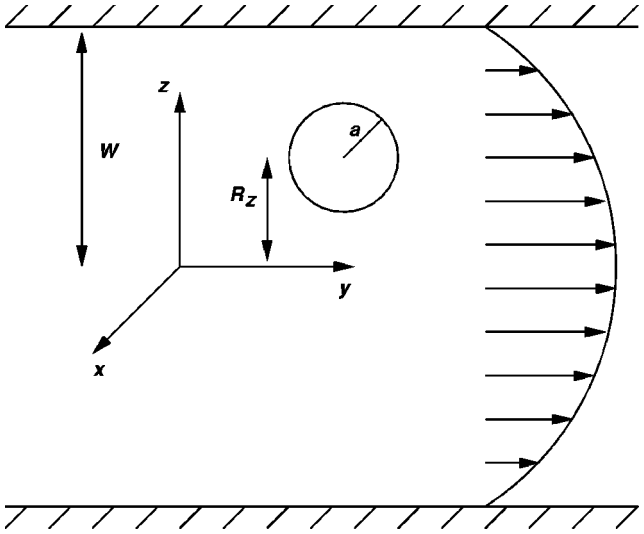

FIG. 1. Parameters and coordinate system for a spherical particle between parallel planar walls.

exact because it reduces the calculation of matrix elements to quadrature, involving one-dimensional integrals that can be calculated numerically to any desired accuracy. By inverting the matrix representation of the Green tensor, we obtain the friction matrix whose elements enable us to find the friction and mobility functions. Moreover, the same method readily generalizes to the N-body case with only minor modifications to the integrals which give the requisite matrix elements. In the present paper we describe this solution technique and obtain all friction and mobility functions for a single particle in Poiseuille flow between two walls.

In Sec. II we use the two-dimensional Fourier transform to derive a symmetric form of the Green tensor for creeping flow between parallel plane walls. In Sec. III we recall the definition of the one-particle friction matrix which describes the force multipoles excited when the particle moves in a Poiseuille flow. In Sec. IV we give an exact expression for the matrix elements of the operator which contains all the wall effects. In Sec. V we define the 13 friction and mobility functions which describe a particle in Poiseuille flow and relate them to the matrix elements of the friction matrix. We also give the Stokesian dynamics equations for the motion of the particle in terms of these friction and mobility functions. In Sec. VI we discuss the numerical calculation of these functions, comparing with earlier results and investigating how the exact results compare with an approximation based on superposition of one-wall results. Finally, in Sec. VII we use the numerical mobilities to carry out a Stokesian dynamics calculation of the motion of a magnetic particle in a Poiseuille flow and subject to an external magnetic field.

II. TWO-WALL GREEN TENSOR

We consider a geometry as shown in Fig. 1 in which the coordinate system is chosen with origin midway between the two parallel hard walls and with $x-y$ axes parallel to the two walls. The positions of the walls are then at $z=\pm W$ where the total gap width between the walls is $2W$. We seek to calculate the Green tensor for the creeping-motion Stokes flow equations describing slow motion of a Newtonian viscous fluid filling the space between the walls and subject to stick boundary conditions at the walls.

The solution to this problem has previously been calculated by Liron and Mochon,[20] but in a rather unsymmetric form using coordinates with the origin located on one wall. The method used there was to start with the Oseen tensor,[21] the Green tensor for Stokes flow in unbounded fluid, and then to sum explicitly a series of its reflections in the two walls. This reflection sum did not completely satisfy the stick boundary conditions, but could be expressed as a two-dimensional Fourier transform of the x and y dependence. The complete Green tensor was expressed as this partial result plus a residual term which satisfied the homogeneous creeping motion equations together with known boundary conditions at the walls. After a two-dimensional transform of the residual term, a set of ordinary differential equations resulted which was solved explicitly.

We have found an alternative method for calculating the Green tensor which starts from the beginning with a two-dimensional Fourier transform and leads, because of the coordinate system we use, to a more symmetric and more manageable expression. In particular, it is well suited to calculating the matrix elements of the Green tensor needed to generate the grand resistance and mobility matrices describing the creeping motion of N hard spheres in suspension between the two walls. Our result is, of course, equivalent to the result of Liron and Mochon and can, with some labor, be shown to be identical with their expressions, taking account of the different choice of coordinate system.

The problem then is to find the solution $\mathbf{T}(\mathbf{r}_1,\mathbf{r}_2)$ to the Stokes equations

$$\begin{aligned}&\eta\nabla_1^2\mathbf{T}(\mathbf{r}_1,\mathbf{r}_2)-\boldsymbol{\nabla}_1\mathbf{Q}(\mathbf{r}_1,\mathbf{r}_2)=-\mathbf{1}\delta(\mathbf{r}_1-\mathbf{r}_2),\\&\boldsymbol{\nabla}_1\cdot\mathbf{T}(\mathbf{r}_1,\mathbf{r}_2)=0,\end{aligned}\tag{1}$$

subject to the boundary condition that $\mathbf{T}$ vanish when the field point $\mathbf{r}_1$ lies on either wall. The source point $\mathbf{r}_2$ is the point where a unit force is applied to the fluid, and η is the Newtonian shear viscosity. In unbounded fluid, $\mathbf{T}(\mathbf{r}_1,\mathbf{r}_2)$ and $\mathbf{Q}(\mathbf{r}_1,\mathbf{r}_2)$ are given by the Oseen tensor $\mathbf{T}_0(\mathbf{r}_1-\mathbf{r}_2)$ and the pressure field $\mathbf{Q}_0(\mathbf{r}_1-\mathbf{r}_2)$, which have the form

$$\mathbf{T}_0(\mathbf{r})=\frac{1}{8\pi\eta r}(\mathbf{1}+\hat{\mathbf{r}}\hat{\mathbf{r}}),\quad \mathbf{Q}_0(\mathbf{r})=\frac{1}{4\pi}\frac{\hat{\mathbf{r}}}{r^2},\tag{2}$$

where $\hat{\mathbf{r}}=\mathbf{r}/r$. As a consequence of the Lorentz reciprocity relation,[21] the Green tensor satisfies the reciprocity condition

$$T_{\alpha\beta}(\mathbf{r}_1,\mathbf{r}_2)=T_{\beta\alpha}(\mathbf{r}_2,\mathbf{r}_1).\tag{3}$$

If a point force $\mathbf{F}$ is applied to the fluid at the source point $\mathbf{r}_2$, the resultant velocity field at field point $\mathbf{r}_1$ is given by

$$\mathbf{v}(\mathbf{r}_1)=\mathbf{T}(\mathbf{r}_1,\mathbf{r}_2)\cdot\mathbf{F},\tag{4}$$

so we may find the components of $\mathbf{T}$ by solving for the velocity field $\mathbf{v}$ arising in each of two special cases: (I) $\mathbf{F}$ parallel to the walls and (II) $\mathbf{F}$ normal to the walls.

We illustrate the method of solution by considering case (I), and then we quote the general result for $\mathbf{T}$. Thus we choose coordinates so that the force density $F_y\mathbf{e}_y\delta(\mathbf{r}_1-\mathbf{r}_2)$,

where $\mathbf{e}_y$ is the unit vector along the y axis, acts at a point on the z axis, $\mathbf{r}_2=(0,0,z_2)$, and we denote the field point by $\mathbf{r}_1=\mathbf{r}=(x,y,z)$. We then solve

$$\eta\nabla^2\mathbf{v}_I(\mathbf{r})-\boldsymbol{\nabla}p_I(\mathbf{r})=-F_y\mathbf{e}_y\delta(\mathbf{r}-\mathbf{r}_2),\quad \boldsymbol{\nabla}\cdot\mathbf{v}_I=0. \tag{5}$$

By translational symmetry we expect $\mathbf{T}(\mathbf{r}_1,\mathbf{r}_2)$ to depend only on the differences x_1-x_2 and y_1-y_2, so we can introduce a two-dimensional Fourier transform in the $x-y$ plane as follows. Introduce two-dimensional position vectors $\mathbf{s}_1=(x_1,y_1)$, $\mathbf{s}_2=(x_2,y_2)$ and a two-dimensional wave vector $\mathbf{q}=(q_x,q_y)$. We then express $\mathbf{T}(\mathbf{r}_1,\mathbf{r}_2)$ as $\mathbf{T}(\mathbf{s}_1-\mathbf{s}_2,z_1,z_2)$ and transform it as

$$\mathbf{T}(\mathbf{r}_1,\mathbf{r}_2)=\mathbf{T}(\mathbf{s}_1-\mathbf{s}_2,z_1,z_2)=\int d\mathbf{q}\,e^{i\mathbf{q}\cdot(\mathbf{s}_1-\mathbf{s}_2)}\hat{\mathbf{T}}(\mathbf{q},z_1,z_2). \tag{6}$$

The reciprocity relation (3) is expressed in $\mathbf{q}$ space as

$$\hat{T}_{\alpha\beta}(\mathbf{q},z_1,z_2)=\hat{T}^*_{\beta\alpha}(\mathbf{q},z_2,z_1), \tag{7}$$

where complex conjugation is now involved.

To solve Eq. (5) for case (I) we write $\mathbf{v}_I(\mathbf{r})=\mathbf{v}_I(\mathbf{s},z)$, where $\mathbf{s}=(x,y)$, and transform all fields as

$$\mathbf{v}_I(\mathbf{s},z)=\int d\mathbf{q}\,\hat{\mathbf{v}}_I(\mathbf{q},z)e^{i\mathbf{q}\cdot\mathbf{s}},$$

$$p_I(\mathbf{s},z)=\int d\mathbf{q}\,\hat{p}_I(\mathbf{q},z)e^{i\mathbf{q}\cdot\mathbf{s}}, \tag{8}$$

$$\delta(\mathbf{r}-\mathbf{r}_2)=\frac{1}{(2\pi)^2}\delta(z-z_2)\int d\mathbf{q}\,e^{i\mathbf{q}\cdot\mathbf{s}}.$$

Inserting these representations into the Stokes equations (5) leads to a coupled system of ordinary differential equations for case (I):

$$\eta\left(\frac{d^2}{dz^2}-q^2\right)\hat{v}_{Ix}(\mathbf{q},z)-iq_x\hat{p}_I(\mathbf{q},z)=0,$$

$$\eta\left(\frac{d^2}{dz^2}-q^2\right)\hat{v}_{Iy}(\mathbf{q},z)-iq_y\hat{p}_I(\mathbf{q},z)=-\frac{F_y}{(2\pi)^2}\delta(z-z_2), \tag{9}$$

$$\eta\left(\frac{d^2}{dz^2}-q^2\right)\hat{v}_{Iz}(\mathbf{q},z)-\frac{d\hat{p}_I(\mathbf{q},z)}{dz}=0,$$

with the divergenceless condition

$$iq_x\hat{v}_{Ix}(\mathbf{q},z)+iq_y\hat{v}_{Iy}(\mathbf{q},z)+\frac{d\hat{v}_{Iz}(\mathbf{q},z)}{dz}=0. \tag{10}$$

To solve this set of equations we first use Eq. (10) together with Eqs. (9) to obtain an equation for the pressure field

$$\left(\frac{d^2}{dz^2}-q^2\right)\hat{p}_I(\mathbf{q},z)=\frac{iq_yF_y}{(2\pi)^2}\delta(z-z_2), \tag{11}$$

where $q^2=\mathbf{q}\cdot\mathbf{q}=q_x^2+q_y^2$. This inhomogeneous equation has the solution

$$\hat{p}_I(\mathbf{q},z)=N_1\cosh qz+N_2\sinh qz-\frac{iq_yF_y}{8\pi^2q}e^{-q|z-z_2|}, \tag{12}$$

where N_1 and N_2 are constants that depend parametrically on z_2. The absolute value $|z-z_2|$ provides the δ-function singularity. Next, insert this form of $\hat{p}_I$ into the equation for $\hat{v}_{Iz}$ and solve for $\hat{v}_{Iz}$ as

$$\hat{v}_{Iz}(\mathbf{q},z)=\frac{1}{2\eta}(N_1z\cosh qz+N_2z\sinh qz+N_3\cosh qz+N_4\sinh qz)-\frac{iq_yF_y}{16\pi^2\eta q}(z-z_2)e^{-q|z-z_2|}, \tag{13}$$

with N_3 and N_4 additional constants. The stick boundary condition means that all velocity components $\hat{v}_{I\alpha}(\mathbf{q},z)$ must vanish at $z=\pm W$. From the divergenceless condition (10) we see that in addition $d\hat{v}_{Iz}/dz$ must also vanish at $z=\pm W$. These four boundary conditions determine $N_1,\ldots,N_4$ uniquely, and hence both $\hat{v}_{Iz}$ and $\hat{p}_I$ are known completely. We next insert the pressure field into Eqs. (9) for $\hat{v}_{Ix}$ and $\hat{v}_{Iy}$ and solve these ordinary differential equations with the stick boundary conditions that $\hat{v}_{Ix}$ and $\hat{v}_{Iy}$ vanish at $z=\pm W$. Thus we have solved case (I) completely for $\hat{\mathbf{v}}_I$ and from Eq. (4) we can read off $\hat{T}_{xy}$, $\hat{T}_{yy}$, and $\hat{T}_{zy}$. Reciprocity and rotational symmetry about the z axis give us $\hat{T}_{yx}$, $\hat{T}_{xx}$, $\hat{T}_{zx}$, and $\hat{T}_{yz}$. To obtain the element $\hat{T}_{zz}$ we repeat the method of solution to obtain the solution $\hat{\mathbf{v}}_{II}$ corresponding to case (II) ($\mathbf{F}=F_z\mathbf{e}_z$). This second calculation gives $\hat{T}_{xz}$ and $\hat{T}_{yz}$ independently of the case (I) calculation, providing a check that the solution obeys the reciprocity condition.

The explicit result for $\hat{\mathbf{T}}$ can be expressed in the following way. Introducing the unit vector $\hat{\mathbf{q}}=\mathbf{q}/q$ alongside the coordinate unit vectors $\mathbf{e}_x$, $\mathbf{e}_y$, and $\mathbf{e}_z$, we write the tensor structure of $\hat{\mathbf{T}}(\mathbf{q},z_1,z_2)$ in dyadic notation as

$$\hat{\mathbf{T}}(\mathbf{q},z_1,z_2)=\frac{1}{16\pi^2\eta q}[t_{nn}(q,z_1,z_2)\mathbf{e}_z\mathbf{e}_z+it_{np}(q,z_1,z_2)\mathbf{e}_z\hat{\mathbf{q}}+it_{pn}(q,z_1,z_2)\hat{\mathbf{q}}\mathbf{e}_z+(i)^2t_{pp}(q,z_1,z_2)\hat{\mathbf{q}}\hat{\mathbf{q}}+r_{pp}(q,z_1,z_2)(\mathbf{1}-\mathbf{e}_z\mathbf{e}_z)], \tag{14}$$

with real scalar functions $t_{nn},\ldots,r_{pp}$. The solution splits naturally into the form

$$\hat{\mathbf{T}}(\mathbf{q},z_1,z_2)=\hat{\mathbf{T}}_0(\mathbf{q},z_1-z_2)+\hat{\mathbf{T}}_1(\mathbf{q},z_1,z_2), \tag{15}$$

corresponding in real-space to

$$\mathbf{T}(\mathbf{r}_1,\mathbf{r}_2)=\mathbf{T}_0(\mathbf{r}_1-\mathbf{r}_2)+\mathbf{T}_1(\mathbf{r}_1,\mathbf{r}_2), \tag{16}$$

with $\mathbf{T}_0$ the Oseen tensor whose two-dimensional Fourier transform $\hat{\mathbf{T}}_0(\mathbf{q},z_1-z_2)$ takes the form (14) with scalar functions $t_{0nn},\ldots,r_{0pp}$ defined as

$$t_{0nn}=t_{0pp}=(1+q|z_1-z_2|)e^{-q|z_1-z_2|},$$

$$t_{0np}=t_{0pn}=-q(z_1-z_2)e^{-q|z_1-z_2|}, \tag{17}$$

$$r_{0pp}=2e^{-q|z_1-z_2|}.$$

The tensor $\hat{\mathbf{T}}_1$ contains all wall-dependent corrections to the infinite-fluid result.

To express $\hat{\mathbf{T}}_1$ we must first introduce some extra notation. We define the dimensionless variables u, v, and w as

$$u=qW, \quad v=qz_2, \quad w=qz_1, \tag{18}$$

and introduce simple auxiliary functions

$$\begin{aligned} &A_{\pm}(u)=u\pm\sinh ue^{-u}, \quad B_{\pm}(u)=u\pm\cosh ue^{-u},\\ &C_{\pm}(u)=u(1+u)\pm\sinh ue^{-u},\\ &D_{\pm}(u)=u(1+u)\pm\cosh ue^{-u},\\ &E_{\pm}(u)=\frac{1}{\sinh u\cosh u\pm u}. \end{aligned} \tag{19}$$

In terms of these functions we find for the scalar functions $t_{1nn},\ldots,r_{1pp}$, corresponding to $\hat{\mathbf{T}}_1$, the following expressions:

$$\begin{aligned} t_{1nn}(q,z_1,z_2)=&-E_-(u)w\cosh wv\cosh v-E_+(u)w\sinh wv\sinh v+E_-(u)B_+(u)(w\cosh w\sinh v+\sinh wv\cosh v)\\ &+E_+(u)A_+(u)(w\sinh w\cosh v+\cosh wv\sinh v)-E_-(u)D_+(u)\sinh w\sinh v\\ &-E_+(u)C_+(u)\cosh w\cosh v, \end{aligned} \tag{20}$$

$$\begin{aligned} t_{1np}(q,z_1,z_2)=&E_-(u)w\cosh wv\sinh v+E_+(u)w\sinh wv\cosh v-E_-(u)B_+(u)\sinh wv\sinh v\\ &-E_+(u)B_-(u)w\sinh w\sinh v-E_-(u)A_-(u)w\cosh w\cosh v-E_+(u)A_+(u)\cosh wv\cosh v\\ &+u^2E_-(u)\sinh w\cosh v+u^2E_+(u)\cosh w\sinh v, \end{aligned} \tag{21}$$

$$\begin{aligned} t_{1pn}(q,z_1,z_2)=&-E_-(u)w\sinh wv\cosh v-E_+(u)w\cosh wv\sinh v+E_-(u)B_+(u)w\sinh w\sinh v\\ &+E_+(u)B_-(u)\sinh wv\sinh v+E_-(u)A_-(u)\cosh wv\cosh v+E_+(u)A_+(u)w\cosh w\cosh v\\ &-u^2E_-(u)\cosh w\sinh v-u^2E_+(u)\sinh w\cosh v, \end{aligned} \tag{22}$$

$$\begin{aligned} t_{1pp}(q,z_1,z_2)=&E_-(u)w\sinh wv\sinh v+E_+(u)w\cosh wv\cosh v-E_+(u)B_-(u)(w\cosh w\sinh v+\sinh wv\cosh v)\\ &-E_-(u)A_-(u)(w\sinh w\cosh v+\cosh wv\sinh v)+E_+(u)D_-(u)\sinh w\sinh v\\ &+E_-(u)C_-(u)\cosh w\cosh v-2u\tanh uE_-(u)\cosh w\cosh v-2u\coth uE_+(u)\sinh w\sinh v, \end{aligned} \tag{23}$$

$$r_{1pp}(q,z_1,z_2)=-\frac{2e^{-u}}{\cosh u}\cosh w\cosh v-\frac{2e^{-u}}{\sinh u}\sinh w\sinh v. \tag{24}$$

One sees from these explicit expressions that t_{1np} and t_{1pn} satisfy the reciprocity relation

$$t_{1np}(q,z_1,z_2)=-t_{1pn}(q,z_2,z_1), \tag{25}$$

which follows from Eqs. (7) and (14).

If we use the expression (14) in the Fourier transform (6) and note that the scalar functions $t_{1nn},\ldots,r_{1pp}$ depend only upon q, we can convert the double integral over q_x and q_y into polar coordinates in $\mathbf{q}$ space, $q_x=q\cos\phi$, $q_y=q\sin\phi$, and then carry out the angular integration over ϕ explicitly. This gives an expression for $\mathbf{T}_1(\mathbf{r}_1,\mathbf{r}_2)$ as a one-dimensional integral over q with Bessel function weights. If we define $s=\sqrt{x^2+y^2}$, we find

$$\begin{aligned} T_{1xx}(\mathbf{r}_1,\mathbf{r}_2)=&-\frac{1}{16\pi\eta}\int_0^\infty dq\left(J_0(qs)+\frac{y^2-x^2}{s^2}J_2(qs)\right)\\ &\times t_{1pp}(q,z_1,z_2)+\frac{1}{8\pi\eta}\int_0^\infty dqJ_0(qs)\\ &\times r_{1pp}(q,z_1,z_2), \end{aligned}$$

$$T_{1zz}(\mathbf{r}_1,\mathbf{r}_2)=\frac{1}{8\pi\eta}\int_0^\infty dqJ_0(qs)t_{1nn}(q,z_1,z_2), \tag{26}$$

$$T_{1xy}(\mathbf{r}_1,\mathbf{r}_2)=\frac{xy}{8\pi\eta}\int_0^\infty dqJ_2(qs)t_{1pp}(q,z_1,z_2),$$

$$T_{1xz}(\mathbf{r}_1,\mathbf{r}_2)=-\frac{1}{8\pi\eta}\frac{x}{s}\int_0^\infty dqJ_1(qs)t_{1pn}(q,z_1,z_2).$$

The component T_{1yy} is the same as T_{1xx} with the change $x\to y$, $y\to -x$, T_{1yz} is the same as T_{1xz} with the factor x replaced by y, and other elements follow by reciprocity. By replacing the functions $t_{1nn},\ldots,r_{1pp}$ with $t_{0nn},\ldots,r_{0pp}$ from Eq. (17) we get a representation of the Oseen tensor $T_{0\alpha\beta}$.

The expressions (20)–(24) are slightly cumbersome to use, so it is useful for later applications to introduce a more compact intermediate notation. We observe that quantities like $t_{1nn},\ldots$ are all bilinear expressions in the four functions $f_k(w)$, $f_k(v)$, $k=1,\ldots,4$, where

$$\begin{aligned} &f_1(v)=\cosh v, \quad f_2(v)=\sinh v,\\ &f_3(v)=v\cosh v, \quad f_4(v)=v\sinh v. \end{aligned} \tag{27}$$

If we regard the four functions $f_k(v)$ as elements of a four-component vector $\mathcal{F}(v)$, then we could express t_{1nn} for example as

$$t_{1nn}=\mathcal{F}^T(w)\cdot\mathcal{E}_{nn}(u)\cdot\mathcal{F}(v), \tag{28}$$

where $\mathcal{F}^T$ is the transpose of vector $\mathcal{F}$, the centerdot indicates 4×4 matrix multiplication with $\mathcal{E}_{nn}(u)$ a 4×4 matrix with elements

$$\mathcal{E}_{nn}(u)=\begin{pmatrix} -E_+(u)C_+(u) & 0 & 0 & E_+(u)A_+(u) \\ 0 & -E_-(u)D_+(u) & E_-(u)B_+(u) & 0 \\ 0 & E_-(u)B_+(u) & -E_-(u) & 0 \\ E_+(u)A_+(u) & 0 & 0 & -E_+(u) \end{pmatrix}. \tag{29}$$

Likewise, all the other terms in Eqs. (21)–(24) can be expressed as

$$t_{1np}=\mathcal{F}^T(w)\cdot\mathcal{E}_{np}(u)\cdot\mathcal{F}(v),\quad t_{1pn}=\mathcal{F}^T(w)\cdot\mathcal{E}_{pn}(u)\cdot\mathcal{F}(v), \tag{30}$$
$$t_{1pp}=\mathcal{F}^T(w)\cdot\mathcal{E}_{pp}(u)\cdot\mathcal{F}(v),\quad r_{1pp}=\mathcal{F}^T(w)\cdot\mathcal{G}_{pp}(u)\cdot\mathcal{F}(v),$$

where the elements of the 4×4 matrices $\mathcal{E}_{np}$, $\mathcal{E}_{pn}$, $\mathcal{E}_{pp}$, and $\mathcal{G}_{pp}$ can be read off the explicit expressions in Eqs. (21)–(24) above. These matrices have the useful symmetry properties

$$\mathcal{E}_{nn}=\mathcal{E}_{nn}^T,\quad \mathcal{E}_{pp}=\mathcal{E}_{pp}^T,\quad \mathcal{E}_{np}=-\mathcal{E}_{pn}^T,\quad \mathcal{G}_{pp}=\mathcal{G}_{pp}^T. \tag{31}$$

III. ONE-PARTICLE FRICTION MATRIX

The Green tensor of the previous section gives the fluid response to a point force applied between two walls. We are ultimately interested in describing the fluid response when there are N extended spherical particles suspended in the fluid between the two walls. Previously, we studied the analogous problem with only one bounding wall and we showed there that knowledge of the Green tensor enables one to obtain a matrix representation of the linear operator that relates the force multipoles excited on the spherical particles to the linear and angular velocities of the spheres and to any incident flow field.[14,15] For simplicity we summarize how these relations arise for the case of one extended spherical particle of radius a suspended in fluid between two walls.

The sphere itself moves with rigid-body translational and angular velocities $\mathbf{U}$ and $\mathbf{\Omega}$ subject to an incident flow field $\mathbf{v}_0(\mathbf{r})$ and $p_0(\mathbf{r})$ which obeys the Stokes equation with stick boundary conditions at the two walls:

$$\eta\nabla^2\mathbf{v}_0(\mathbf{r})-\nabla p_0(\mathbf{r})=0,\quad \nabla\cdot\mathbf{v}_0(\mathbf{r})=0. \tag{32}$$

When the spherical particle is present in this flow, it perturbs it by exerting a force density on the fluid, $\mathbf{F}(\mathbf{r})$, which is localized on the particle surface where stick boundary conditions apply. The exact perturbed flow in the presence of the particle can then be expressed using the Green tensor as

$$\mathbf{v}(\mathbf{r}_1)=\mathbf{v}_0(\mathbf{r}_1)+\int\mathbf{T}(\mathbf{r}_1,\mathbf{r}_2)\cdot\mathbf{F}(\mathbf{r}_2)d\mathbf{r}_2, \tag{33}$$

where $\mathbf{F}(\mathbf{r}_2)$ acts at the particle surface and the field $\mathbf{v}(\mathbf{r}_1)$ is formally defined in all of the space between the two walls by requiring it to be equal to the rigid-body velocity of the sphere inside the particle. Thus, if the sphere is located with its center at $\mathbf{R}$, then, for $|\mathbf{r}_1-\mathbf{R}|\leqslant a$,

$$\mathbf{v}(\mathbf{r}_1)=\mathbf{u}(\mathbf{r}_1)=\mathbf{U}+\mathbf{\Omega}\times(\mathbf{r}_1-\mathbf{R}). \tag{34}$$

We can reduce the integral equation (33) to a set of linear algebraic equations by expanding the various functions involved there into a complete set of solutions to the homogeneous Stokes equations (32). There are two sets of such functions[15] $\mathbf{v}^+_{\ell m\sigma}(\mathbf{r})$ and $\mathbf{v}^-_{\ell m\sigma}(\mathbf{r})$, where $\ell m\sigma$ take the values $\ell=1, 2, 3,...$, $m=-\ell,-\ell+1,...,\ell-1,\ell$, and $\sigma=0, 1, 2$. The solutions $\mathbf{v}^+_{\ell m\sigma}(\mathbf{r})$ are regular at $\mathbf{r}=0$ and grow at infinity, while the $\mathbf{v}^-_{\ell m\sigma}(\mathbf{r})$ are singular at $\mathbf{r}=0$ and vanish at infinity. In terms of these functions we can expand the Oseen tensor $\mathbf{T}_0(\mathbf{r}_1-\mathbf{r}_2)$ about the center of the sphere at point $\mathbf{R}$ as[15]

$$\mathbf{T}_0(\mathbf{r}_1-\mathbf{r}_2)=\frac{1}{\eta}\sum_{\ell m\sigma}\mathbf{v}^-_{\ell m\sigma}(\mathbf{r}_>)\mathbf{v}^{+*}_{\ell m\sigma}(\mathbf{r}_<), \tag{35}$$

where $\mathbf{r}_>$ and $\mathbf{r}_<$ refer, respectively, to the larger and smaller of the relative position vectors $\mathbf{r}_1-\mathbf{R}$ and $\mathbf{r}_2-\mathbf{R}$. Since the Oseen tensor $\mathbf{T}_0(\mathbf{r}_1-\mathbf{r}_2)$ contains all the singularities at $\mathbf{r}_1-\mathbf{r}_2=0$, $\mathbf{T}_1(\mathbf{r}_1,\mathbf{r}_2)$ can be expanded similarly, but using only the regular functions $\mathbf{v}^+_{\ell m\sigma}$:

$$\mathbf{T}_1(\mathbf{r}_1,\mathbf{r}_2)=\sum_{\ell_1m_1\sigma_1}\sum_{\ell_2m_2\sigma_2}T_1(\ell_1m_1\sigma_1,\ell_2m_2\sigma_2)\times\mathbf{v}^+_{\ell_1m_1\sigma_1}(\mathbf{r}_1-\mathbf{R})\mathbf{v}^{+*}_{\ell_2m_2\sigma_2}(\mathbf{r}_2-\mathbf{R}). \tag{36}$$

Because of the stick boundary conditions, we know the value of $\mathbf{v}(\mathbf{r}_1)$ on the surface of the particle from Eq. (34), $\mathbf{v}(\mathbf{r}_1)-\mathbf{v}_0(\mathbf{r}_1)=\mathbf{u}(\mathbf{r}_1)-\mathbf{v}_0(\mathbf{r}_1)$, so we can expand this difference of fields in terms of the regular solutions centered on $\mathbf{R}$:

$$\mathbf{u}(\mathbf{r}_1)-\mathbf{v}_0(\mathbf{r}_1)=\sum_{\ell m\sigma}c(\ell m\sigma)\mathbf{v}^+_{\ell m\sigma}(\mathbf{r}_1-\mathbf{R}). \tag{37}$$

The expansion coefficients above such as $c(\ell m\sigma)$ can be calculated using adjoint sets of functions[15,22] $\mathbf{w}^{\pm}_{\ell m\sigma}(\mathbf{r})$, which, together with $\mathbf{v}^{\pm}_{\ell m\sigma}(\mathbf{r})$, form biorthonormal sets on the surface of a sphere of arbitrary radius b in the sense that

$$\int\mathbf{w}^{\pm *}_{\ell_1m_1\sigma_1}(\mathbf{r})\frac{1}{b}\delta(r-b)\cdot\mathbf{v}^{\pm}_{\ell_2m_2\sigma_2}(\mathbf{r})d\mathbf{r}=\delta_{\ell_1\ell_2}\delta_{m_1m_2}\delta_{\sigma_1\sigma_2}. \tag{38}$$

We can simplify notation by introducing a scalar product $\langle \mathbf{f}|\mathbf{g}\rangle$ defined for any two complex valued vector fields $\mathbf{f}(\mathbf{r})$ and $\mathbf{g}(\mathbf{r})$ as

$$\langle \mathbf{f}|\mathbf{g}\rangle = \int \mathbf{f}^*(\mathbf{r})\cdot\mathbf{g}(\mathbf{r})d\mathbf{r}. \tag{39}$$

With this notation we express Eq. (38) as

$$\langle \mathbf{w}^{\pm}_{\ell_1 m_1\sigma_1}\delta_b|\mathbf{v}^{\pm}_{\ell_2 m_2\sigma_2}\rangle = \delta_{\ell_1\ell_2}\delta_{m_1 m_2}\delta_{\sigma_1\sigma_2}, \tag{40}$$

where δ_b is shorthand for $(1/b)\delta(r-b)$. The coefficients $c(\ell m\sigma)$ are then

$$c(\ell m\sigma) = \langle \mathbf{w}^{+}_{\ell m\sigma}\delta_a|\mathbf{u}-\mathbf{v}_0\rangle, \tag{41}$$

where $\mathbf{w}^{+}_{\ell m\sigma}$ is understood to be centered at $\mathbf{R}$, $\mathbf{w}^{+}_{\ell m\sigma}(\mathbf{r}-\mathbf{R})$, and δ_a is shorthand for $(1/a)\delta(|\mathbf{r}-\mathbf{R}|-a)$.

Using the results above, we reexpress the integral equation (33) as

$$c(\ell_1 m_1\sigma_1) = \sum_{\ell_2 m_2\sigma_2} M(\ell_1 m_1\sigma_1,\ell_2 m_2\sigma_2) f(\ell_2 m_2\sigma_2), \tag{42}$$

where $f(\ell m\sigma)$ is a force multipole of order $\ell m\sigma$ defined as

$$f(\ell m\sigma) = \langle \mathbf{v}^{+}_{\ell m\sigma}|\mathbf{F}\rangle = \int \mathbf{v}^{+}_{\ell m\sigma}(\mathbf{r}-\mathbf{R})\cdot\mathbf{F}(\mathbf{r})d\mathbf{r}. \tag{43}$$

The linear relation (42) can be expressed as a matrix equation involving infinite-dimensional vectors c and f with elements $c(\ell m\sigma)$ and $f(\ell m\sigma)$ and an infinite-dimensional matrix M with elements $M(\ell_1 m_1\sigma_1,\ell_2 m_2\sigma_2)$. In this compact notation M takes the form

$$\mathsf{M} = \mathsf{Z}_0^{-1} + \mathsf{T}_1. \tag{44}$$

Here Z_0^{-1} is the inverse friction matrix for a single sphere in unbounded fluid[15,22] calculated from the Oseen tensor $\mathbf{T}_0(\mathbf{r}_1-\mathbf{r}_2)$ as

$$Z_0^{-1}(\ell_1 m_1\sigma_1,\ell_2 m_2\sigma_2) = \langle \mathbf{w}^{+}_{\ell_1 m_1\sigma_1}\delta_a|\mathbf{T}_0|\mathbf{w}^{+}_{\ell_2 m_2\sigma_2}\delta_a\rangle, \tag{45}$$

And T_1 is the matrix calculated from the wall-dependent part of the Green tensor $\mathbf{T}_1$ defined in Eq. (15):

$$T_1(\ell_1 m_1\sigma_1,\ell_2 m_2\sigma_2) = \langle \mathbf{w}^{+}_{\ell_1 m_1\sigma_1}\delta_a|\mathbf{T}_1|\mathbf{w}^{+}_{\ell_2 m_2\sigma_2}\delta_a\rangle. \tag{46}$$

The linear equation (42) can be written

$$\mathsf{c} = \mathsf{M}\cdot\mathsf{f}, \tag{47}$$

and the force multipole vector f is obtained as

$$\mathsf{f} = \mathsf{Z}\cdot\mathsf{c}, \quad \mathsf{Z} = \mathsf{M}^{-1}, \tag{48}$$

where Z is the friction matrix for a sphere between two walls. In terms of Z we reexpress Eq. (44) as

$$\mathsf{Z}^{-1} = \mathsf{Z}_0^{-1} + \mathsf{T}_1. \tag{49}$$

IV. MATRIX ELEMENTS OF T_1

To obtain the friction matrix Z from Eq. (49), we must first calculate the matrix T_1 as defined in Eq. (46). This can be done using the $\mathbf{q}$-space form of $\hat{\mathbf{T}}_1(\mathbf{q},z_1,z_2)$ as given in Eq. (14) with the explicit scalar functions $t_{1nn},\ldots,r_{1pp}$ given in Eqs. (20)–(24). To explain how the calculation is carried out, first recall that in the integrations involved in the matrix element $T_1(\ell_1 m_1\sigma_1,\ell_2 m_2\sigma_2)$ both functions $\mathbf{w}^{+}_{\ell_1 m_1\sigma_1}$ and $\mathbf{w}^{+}_{\ell_2 m_2\sigma_2}$ are centered on the sphere center located at $\mathbf{R}$ and are localized to the sphere surface by the delta function denoted δ_a. Thus the integrations over $\mathbf{r}_1$ and $\mathbf{r}_2$ can be expressed as integrations over $\boldsymbol{\epsilon}_1=\mathbf{r}_1-\mathbf{R}$ and $\boldsymbol{\epsilon}_2=\mathbf{r}_2-\mathbf{R}$, where both $\boldsymbol{\epsilon}_1$ and $\boldsymbol{\epsilon}_2$ are restricted to have constant length a. If we introduce the two-dimensional vectors $\boldsymbol{\Delta}_1=(\epsilon_{1x},\epsilon_{1y})$ and $\boldsymbol{\Delta}_2=(\epsilon_{2x},\epsilon_{2y})$, we can write $\mathbf{T}_1(\mathbf{r}_1,\mathbf{r}_2)$ as

$$\mathbf{T}_1(\mathbf{r}_1,\mathbf{r}_2) = \int d\mathbf{q}\, e^{i\mathbf{q}\cdot\boldsymbol{\Delta}_1}\hat{\mathbf{T}}_1(\mathbf{q},z_1,z_2)e^{-i\mathbf{q}\cdot\boldsymbol{\Delta}_2}, \tag{50}$$

where $z_1=R_z+\epsilon_{1z}$ and $z_2=R_z+\epsilon_{2z}$. The dependence of $\hat{\mathbf{T}}_1$ on z_1 and z_2 is through products of functions like $f_j(w)f_k(v)$ where $w=qz_1=qR_z+q\epsilon_{1z}=qR_z+w_1$ and $v=qz_2=qR_z+q\epsilon_{2z}=qR_z+v_2$. Using addition theorems for hyperbolic functions enables one to express $f_j(v)$ in terms of the $f_k(v_2)$ with R_z-dependent coefficient functions. This relation is most easily expressed in the matrix notation introduced at the end of Sec. II. Thus the vector $\mathcal{F}(v)$ is related to $\mathcal{F}(v_2)$ by a matrix operation

$$\mathcal{F}(v) = \mathcal{M}(\rho)\cdot\mathcal{F}(v_2), \tag{51}$$

where $\rho=qR_z$ and the matrix has the form

$$\mathcal{M}(\rho) = \begin{pmatrix} f_1(\rho) & f_2(\rho) & 0 & 0 \\ f_2(\rho) & f_1(\rho) & 0 & 0 \\ f_3(\rho) & f_4(\rho) & f_1(\rho) & f_2(\rho) \\ f_4(\rho) & f_3(\rho) & f_2(\rho) & f_1(\rho) \end{pmatrix}. \tag{52}$$

Each term in $\hat{\mathbf{T}}_1$—for example, t_{1nn}—can then be expressed in the form

$$t_{1nn} = \mathcal{F}^T(w_1)\cdot\mathcal{M}^T(\rho)\cdot\mathcal{E}_{nn}(u)\cdot\mathcal{M}(\rho)\cdot\mathcal{F}(v_2). \tag{53}$$

Thus from Eqs. (14), (28), (30), and (51) we find that $\hat{\mathbf{T}}_1$ is a sum of terms, each of which is separable in the variables w_1 and v_2, while the $\boldsymbol{\Delta}_1$ and $\boldsymbol{\Delta}_2$ dependence in Eq. (50) is already separable, so the calculation of the matrix element reduces to a product of integrals, one over $\boldsymbol{\epsilon}_1$ and one over $\boldsymbol{\epsilon}_2$.

Because of the tensor structure of $\mathbf{T}_1$ in real space as given in Eq. (14), there are three sorts of integral to be done. The first type is

$$I^{(k)}_{\ell m\sigma}(\mathbf{q}) = \int d\boldsymbol{\epsilon}_2\mathbf{e}_z\cdot\mathbf{w}^{+}_{\ell m\sigma}(\boldsymbol{\epsilon}_2)\frac{1}{a}\delta(\epsilon_2-a)e^{-i\mathbf{q}\cdot\boldsymbol{\Delta}_2}f_k(v_2)$$

$$= a\int d\Omega_2\mathbf{e}_z\cdot\mathbf{w}^{+}_{\ell m\sigma}(\boldsymbol{\epsilon}_2)e^{-i\mathbf{q}\cdot\boldsymbol{\Delta}_2}f_k(v_2), \tag{54}$$

where the final integral is an angular integration over the direction of vector $\boldsymbol{\epsilon}_2$. The functions $f_k(v_2)$ are as defined in Eqs. (27). The second type of integral is

$$J^{(k)}_{\ell m\sigma}(\mathbf{q}) = a\int d\Omega_2\hat{\mathbf{q}}\cdot\mathbf{w}^{+}_{\ell m\sigma}(\boldsymbol{\epsilon}_2)e^{-i\mathbf{q}\cdot\boldsymbol{\Delta}_2}f_k(v_2). \tag{55}$$

The third type of integral arises from the tensor $\mathbf{1}-\mathbf{e}_z\mathbf{e}_z$, which may also be written as $\hat{\mathbf{q}}\hat{\mathbf{q}}+(\hat{\mathbf{q}}\times\mathbf{e}_z)(\hat{\mathbf{q}}\times\mathbf{e}_z)$. Thus we need also the integral

$$H^{(k)}_{\ell m\sigma}(\mathbf{q}) = a\int d\Omega_2 \hat{\mathbf{q}}\cdot[\mathbf{e}_z\times\mathbf{w}^{+}_{\ell m\sigma}(\boldsymbol{\epsilon}_2)]e^{-i\mathbf{q}\cdot\boldsymbol{\Delta}_2}f_k(v_2). \tag{56}$$

The quantities $I^{(k)}_{\ell m\sigma}(\mathbf{q})$, $J^{(k)}_{\ell m\sigma}(\mathbf{q})$, and $H^{(k)}_{\ell m\sigma}(\mathbf{q})$ for $k=1,...,4$ can be thought of as the components of four-component vectors denoted as $\mathcal{I}_{\ell m\sigma}(\mathbf{q})$, $\mathcal{J}_{\ell m\sigma}(\mathbf{q})$, and $\mathcal{H}_{\ell m\sigma}(\mathbf{q})$, respectively. Using the four-component vector notation introduced at the end of Sec. II, we express the matrix elements of the kernel $\mathbf{T}_1$ as

$$T_1(\ell_1 m_1\sigma_1,\ell_2 m_2\sigma_2) = \int d\mathbf{q}\,\hat{T}_1(\ell_1 m_1\sigma_1,\ell_2 m_2\sigma_2,\mathbf{q}), \tag{57}$$

where

$$\begin{aligned}\hat{T}_1(\ell_1 m_1\sigma_1,\ell_2 m_2\sigma_2,\mathbf{q}) = \frac{1}{16\pi^2\eta q}\{&\mathcal{I}^{T*}_{\ell_1 m_1\sigma_1}(\mathbf{q})\cdot\mathcal{M}^T(\rho)\cdot\mathcal{E}_{nn}(u)\cdot\mathcal{M}(\rho)\cdot\mathcal{I}_{\ell_2 m_2\sigma_2}(\mathbf{q}) + i\mathcal{I}^{T*}_{\ell_1 m_1\sigma_1}(\mathbf{q})\cdot\mathcal{M}^T(\rho)\cdot\mathcal{E}_{np}(u)\\ &\cdot\mathcal{M}(\rho)\cdot\mathcal{J}_{\ell_2 m_2\sigma_2}(\mathbf{q}) + i\mathcal{J}^{T*}_{\ell_1 m_1\sigma_1}(\mathbf{q})\cdot\mathcal{M}^T(\rho)\cdot\mathcal{E}_{pn}(u)\cdot\mathcal{M}(\rho)\cdot\mathcal{I}_{\ell_2 m_2\sigma_2}(\mathbf{q}) + \mathcal{J}^{T*}_{\ell_1 m_1\sigma_1}(\mathbf{q})\cdot\mathcal{M}^T(\rho)\\ &\cdot[\mathcal{G}_{pp}(u)-\mathcal{E}_{pp}(u)]\cdot\mathcal{M}(\rho)\cdot\mathcal{J}_{\ell_2 m_2\sigma_2}(\mathbf{q}) + \mathcal{H}^{T*}_{\ell_1 m_1\sigma_1}(\mathbf{q})\cdot\mathcal{M}^T(\rho)\cdot\mathcal{G}_{pp}(u)\cdot\mathcal{M}(\rho)\cdot\mathcal{H}_{\ell_2 m_2\sigma_2}(\mathbf{q})\}.\end{aligned} \tag{58}$$

This compact expression makes clear where the dependences on the sphere position R_z ($\rho = qR_z$) and the wall separation W ($u = qW$) appear. By combining Eqs. (57) and (58) with the symmetry properties given in Eqs. (31), it follows at once that T_1 is a Hermitian matrix:

$$T_1^*(\ell_2 m_2\sigma_2,\ell_1 m_1\sigma_1) = T_1(\ell_1 m_1\sigma_1,\ell_2 m_2\sigma_2). \tag{59}$$

The derivation of explicit expressions for $\mathcal{I}_{\ell m\sigma}$, $\mathcal{J}_{\ell m\sigma}$, and $\mathcal{H}_{\ell m\sigma}$ is laborious, but hinges upon a simple observation. From the definition of the $\mathbf{w}^{+}_{\ell m\sigma}$ given in Appendix A, it follows that $\mathbf{e}_z\cdot\mathbf{w}^{+}_{\ell m\sigma}$, $\hat{\mathbf{q}}\cdot\mathbf{w}^{+}_{\ell m\sigma}$, and $\hat{\mathbf{q}}\cdot(\mathbf{e}_z\times\mathbf{w}^{+}_{\ell m\sigma})$ are each expressible as linear combinations of spherical harmonics $Y_{\ell_1 m_1}(\hat{\boldsymbol{\epsilon}}_2)$. Recalling that the functions $f_k(v_2)$ defined in Eqs. (26) are linear combinations of $\exp(\pm q\epsilon_{2z})$, we see that the integrations in Eqs. (54–56) can be reduced to a sum of four basic angular integrals of the form

$$K^{\pm}_{\ell_1 m_1}(\mathbf{q}) = a\int d\Omega_2 Y_{\ell_1 m_1}(\hat{\boldsymbol{\epsilon}}_2)e^{-i\mathbf{q}\cdot\boldsymbol{\Delta}_2}e^{\pm q\epsilon_{2z}}, \tag{60}$$

$$L^{\pm}_{\ell_1 m_1}(\mathbf{q}) = qa\int d\Omega_2 Y_{\ell_1 m_1}(\hat{\boldsymbol{\epsilon}}_2)e^{-i\mathbf{q}\cdot\boldsymbol{\Delta}_2}\epsilon_{2z}e^{\pm q\epsilon_{2z}}. \tag{61}$$

As explained in Appendix A, these integrations can be done in terms of solid harmonics. Thus we find

$$K^{\pm}_{\ell_1 m_1}(\mathbf{q}) = \frac{4\pi a^{\ell_1+1}}{(2\ell_1+1)!!}e^{-i\ell_1\pi/2}\mathcal{Y}_{\ell_1 m_1}(q_x,q_y,\pm iq), \tag{62}$$

where $\mathcal{Y}_{\ell_1 m_1}(q_x,q_y,\pm iq)$ is the solid harmonic $\mathcal{Y}_{\ell_1 m_1}(\mathbf{r}) = \mathcal{Y}_{\ell_1 m_1}(x,y,z) = r^{\ell}Y_{\ell_1 m_1}(\hat{\mathbf{r}})$ evaluated at $x=q_x$, $y=q_y$, and $z=\pm iq$. At these complex values of its argument the solid harmonic itself takes the value

$$\mathcal{Y}_{\ell_1 m_1}(q_x,q_y,\pm iq) = \frac{q^{\ell_1}(2\ell_1-1)!!}{n_{\ell_1 m_1}(\ell_1-m_1)!}e^{\pm i(\ell_1+m_1)\pi/2}e^{im_1\phi}, \tag{63}$$

where $q_x = q\cos\phi$, $q_y = q\sin\phi$, and $n_{\ell_1 m_1}$ is a normalization constant:

$$n_{\ell m} = \left(\frac{4\pi}{2\ell+1}\frac{(\ell+m)!}{(\ell-m)!}\right)^{1/2}. \tag{64}$$

For the more complicated integral $L^{\pm}_{\ell_1 m_1}(\mathbf{q})$ we find

$$\begin{aligned}L^{-}_{\ell_1 m_1}(\mathbf{q}) = &\frac{4\pi a(-1)^{\ell_1+1}}{n_{\ell_1 m_1}(2\ell_1+1)(\ell_1-m_1)!}e^{-im_1\pi/2}\\ &\times\left(\frac{(\ell_1^2-m_1^2)}{2\ell_1-1}(qa)^{\ell_1} + \frac{(qa)^{\ell_1+2}}{2\ell_1+3}\right)e^{im_1\phi},\end{aligned} \tag{65}$$

with

$$L^{+}_{\ell_1 m_1}(\mathbf{q}) = (-1)^{(\ell_1+m_1+1)}L^{-}_{\ell_1 m_1}(\mathbf{q}). \tag{66}$$

From Eqs. (62) and (63) we have also

$$K^{+}_{\ell_1 m_1}(\mathbf{q}) = (-1)^{(\ell_1+m_1)}K^{-}_{\ell_1 m_1}(\mathbf{q}). \tag{67}$$

Using these expressions, we evaluate $\hat{T}_1(\ell_1 m_1\sigma_1, \ell_2 m_2\sigma_2,\mathbf{q})$. There remains then in Eq. (57) a two-dimensional integration over $\mathbf{q}$. If we use polar coordinates $q_x = q\cos\phi$, $q_y = q\sin\phi$, and $d\mathbf{q} = q\,dq\,d\phi$ in the two-dimensional $\mathbf{q}$ space, the integration over the angular variable ϕ vanishes unless $m_1 = m_2$ because each of the $\mathcal{I}_{\ell m\sigma}$, $\mathcal{J}_{\ell m\sigma}$, and $\mathcal{H}_{\ell m\sigma}$ depends on ϕ only through a factor $e^{im\phi}$. There remains then a single integration to be done with respect to the magnitude q, giving a matrix T_1 which is diagonal in m_1 and m_2:

$$T_1(\ell_1 m_1\sigma_1,\ell_2 m_2\sigma_2) = \delta_{m_1 m_2}T_1(\ell_1 m_1\sigma_1,\ell_2 m_1\sigma_2). \tag{68}$$

A careful look at the quantities $\mathcal{I}_{\ell m\sigma}$, $\mathcal{J}_{\ell m\sigma}$, and $\mathcal{H}_{\ell m\sigma}$ as given in Appendix B combined with the form of Eq. (58) shows that when $m_1 = m_2$ the matrix elements $T_1(\ell_1 m_1\sigma_1,\ell_2 m_1\sigma_2)$ are real and, because of the Hermitic-

ity (59), they are symmetric in $\ell_1\sigma_1$ and $\ell_2\sigma_2$. These properties of T_1 are shared by Z_0^{-1} and hence by the full friction matrix Z. In addition, one can show that for $m_1=0$, $Z(\ell_1 0\sigma_1,\ell_2 0\sigma_2)$ vanishes unless σ_1 and σ_2 are either both even or both odd.

V. FRICTION AND MOBILITY IN POISEUILLE FLOW

From the results of Sec. IV we can calculate all elements of the matrix T_1 and by use of the explicit expression[15] for Z_0^{-1} we obtain all elements of M and the friction matrix Z. From Z we can obtain all force multipole elements $f(\ell m\sigma)$ excited by the rigid-body motion $\mathbf{u}(\mathbf{r})$ and the incident flow field $\mathbf{v}_0(\mathbf{r})$. In the case of unbounded fluid or fluid bounded by a single hard wall, linear flows $\mathbf{v}_0$, such as simple shear flow, are the simplest flows to study. However, with two fixed hard walls, linear flows cannot satisfy the stick boundary conditions on the two walls, so the simplest incident flow in the present geometry is Poiseuille flow driven by a constant-pressure gradient which we take to be in the y direction. This flow has the form

$$\mathbf{v}_0(\mathbf{r})=\frac{g}{2\eta}(W^2-z^2)\mathbf{e}_y, \quad p_0(\mathbf{r})=-gy. \tag{69}$$

The elements $Z(\ell_1 m_1\sigma_1,\ell_2 m_2\sigma_2)$ for $\ell=1$ and $\sigma=0$, 1 are particularly important because they define the linear relation between the force and torque exerted on the fluid by the particle and the particle translational and angular velocities relative to the fluid. The projection of Z onto this six-dimensional subspace we call the one-particle resistance matrix denoted as

$$\boldsymbol{\zeta}=\mathsf{P}\cdot\mathsf{Z}\cdot\mathsf{P}, \tag{70}$$

where P projects onto the six states $\ell=1$, $m=-1$, 0, 1, and $\sigma=0$, 1. In addition to the representation of $\boldsymbol{\zeta}$ in the spherical harmonic basis, there is also a representation in terms of Cartesian vectors and tensors.[13] If the particle is located at $\mathbf{R}$, the Cartesian representation leads to relations like

$$\begin{pmatrix}\mathbf{F}_1\\ \mathbf{T}_1\end{pmatrix}=-\begin{pmatrix}\boldsymbol{\zeta}^{\mathrm{tt}} & \boldsymbol{\zeta}^{\mathrm{tr}}\\ \boldsymbol{\zeta}^{\mathrm{rt}} & \boldsymbol{\zeta}^{\mathrm{rr}}\end{pmatrix}\begin{pmatrix}\mathbf{v}_0(\mathbf{R})-\mathbf{U}\\ \boldsymbol{\omega}_0(\mathbf{R})-\boldsymbol{\Omega}\end{pmatrix}, \tag{71}$$

where $\boldsymbol{\omega}_0(\mathbf{R})$ is the vorticity of the flow $\mathbf{v}_0$ at the point $\mathbf{R}$:

$$\boldsymbol{\omega}_0(\mathbf{R})=\frac{1}{2}\boldsymbol{\nabla}\times\mathbf{v}_0(\mathbf{R}). \tag{72}$$

The $\boldsymbol{\zeta}^{\mathrm{ab}}$ are Cartesian friction tensors, $\mathbf{F}_1$ and $\mathbf{T}_1$ are the force and torque exerted by the particle on the fluid, and the superscripts t and r correspond respectively to $\ell=1$, $\sigma=0$ and $\ell=1$, $\sigma=1$ in the spherical basis. The one-particle mobility matrix in the Cartesian representation is defined by the inversion of relation (71):

$$\begin{pmatrix}\mathbf{v}_0(\mathbf{R})-\mathbf{U}\\ \boldsymbol{\omega}_0(\mathbf{R})-\boldsymbol{\Omega}\end{pmatrix}=-\begin{pmatrix}\boldsymbol{\mu}^{\mathrm{tt}} & \boldsymbol{\mu}^{\mathrm{tr}}\\ \boldsymbol{\mu}^{\mathrm{rt}} & \boldsymbol{\mu}^{\mathrm{rr}}\end{pmatrix}\begin{pmatrix}\mathbf{F}_1\\ \mathbf{T}_1\end{pmatrix}, \tag{73}$$

where

$$\boldsymbol{\mu}=\begin{pmatrix}\boldsymbol{\mu}^{\mathrm{tt}} & \boldsymbol{\mu}^{\mathrm{tr}}\\ \boldsymbol{\mu}^{\mathrm{rt}} & \boldsymbol{\mu}^{\mathrm{rr}}\end{pmatrix}=\begin{pmatrix}\boldsymbol{\zeta}^{\mathrm{tt}} & \boldsymbol{\zeta}^{\mathrm{tr}}\\ \boldsymbol{\zeta}^{\mathrm{rt}} & \boldsymbol{\zeta}^{\mathrm{rr}}\end{pmatrix}^{-1}=\boldsymbol{\zeta}^{-1}. \tag{74}$$

As noted earlier, because T_1 is diagonal in the m labels, it is real and symmetric, which is also true of Z. Thus $\boldsymbol{\zeta}$ and $\boldsymbol{\mu}$ are also real and symmetric in either the Cartesian or spherical basis.

If there is no external flow, $\mathbf{v}_0=0$, then the only nonvanishing $c(\ell m\sigma)$ correspond to $\ell=1$ and $\sigma=0$, 1. However, for quadratic flow there are other nonvanishing components. Thus the vorticity $\boldsymbol{\omega}_0$ corresponds to $c(1m1)$ and there is the symmetric rate of strain tensor $\mathbf{g}_0(\mathbf{R})$ corresponding to $c(2m0)$:

$$g_{0\mu\nu}(\mathbf{R})=\frac{1}{2}[\boldsymbol{\nabla}_\mu v_{0\nu}(\mathbf{R})+\boldsymbol{\nabla}_\nu v_{0\mu}(\mathbf{R})], \tag{75}$$

where we use Greek subscripts for Cartesian vector and tensor components. Poiseuille flow has additional nonzero elements $c(1m2)$, $c(2m1)$, and $c(3m0)$ which arise from the irreducible components of the third-rank Cartesian tensor $\mathbf{h}_0(\mathbf{R})$:

$$h_{0\alpha\mu\nu}(\mathbf{R})=\frac{1}{2}\boldsymbol{\nabla}_\mu\boldsymbol{\nabla}_\nu v_{0\alpha}(\mathbf{R}). \tag{76}$$

In Cartesian representation there are three irreducible tensors $\mathbf{h}_0^{(1)}$, $\mathbf{h}_0^{(2)}$, and $\mathbf{h}_0^{(3)}$ that arise from $\mathbf{h}_0$ and they are

$$\begin{aligned}
h_{0\mu}^{(1)}&=\frac{1}{2}\nabla^2 v_{0\mu}(\mathbf{R}),\\
h_{0\rho\tau,\gamma}^{(2)}&=\frac{1}{2}(h_{0\rho\tau\gamma}-h_{0\tau\rho\gamma})-\frac{1}{4}(\delta_{\tau\gamma}h_{0\rho}^{(1)}-\delta_{\rho\gamma}h_{0\tau}^{(1)}),\\
h_{0\rho\tau\gamma}^{(3)}&=\frac{1}{3}(h_{0\rho\tau\gamma}+h_{0\tau\gamma\rho}+h_{0\gamma\rho\tau})\\
&\quad-\frac{1}{15}(\delta_{\rho\tau}h_{0\gamma}^{(1)}+\delta_{\tau\gamma}h_{0\rho}^{(1)}+\delta_{\gamma\rho}h_{0\tau}^{(1)}).
\end{aligned} \tag{77}$$

In terms of these tensors $\mathbf{g}_0$ and $\mathbf{h}_0^{(i)}$, the relation (71) is extended to

$$\begin{aligned}
\mathbf{F}_1&=-\boldsymbol{\zeta}^{\mathrm{tt}}\cdot[\mathbf{v}_0(\mathbf{R})-\mathbf{U}]-\boldsymbol{\zeta}^{\mathrm{tr}}\cdot[\boldsymbol{\omega}_0(\mathbf{R})-\boldsymbol{\Omega}]-\boldsymbol{\zeta}^{\mathrm{td}}\cdot\mathbf{g}_0\\
&\quad-\boldsymbol{\zeta}_1^{\mathrm{th}}\cdot\mathbf{h}_0^{(1)}-\boldsymbol{\zeta}_2^{\mathrm{th}}\cdot\mathbf{h}_0^{(2)}-\boldsymbol{\zeta}_3^{\mathrm{th}}\cdot\mathbf{h}_0^{(3)},\\
\mathbf{T}_1&=-\boldsymbol{\zeta}^{\mathrm{rt}}\cdot[\mathbf{v}_0(\mathbf{R})-\mathbf{U}]-\boldsymbol{\zeta}^{\mathrm{rr}}\cdot[\boldsymbol{\omega}_0(\mathbf{R})-\boldsymbol{\Omega}]-\boldsymbol{\zeta}^{\mathrm{rd}}\cdot\mathbf{g}_0\\
&\quad-\boldsymbol{\zeta}_1^{\mathrm{rh}}\cdot\mathbf{h}_0^{(1)}-\boldsymbol{\zeta}_2^{\mathrm{rh}}\cdot\mathbf{h}_0^{(2)}-\boldsymbol{\zeta}_3^{\mathrm{rh}}\cdot\mathbf{h}_0^{(3)}.
\end{aligned} \tag{78}$$

By use of the mobility matrix $\boldsymbol{\mu}$ we can solve for $\mathbf{U}$ and $\boldsymbol{\Omega}$ as in Eq. (73):

$$\begin{aligned}
\mathbf{U}&=\mathbf{v}_0(\mathbf{R})+\boldsymbol{\mu}^{\mathrm{tt}}\cdot\mathbf{F}_1+\boldsymbol{\mu}^{\mathrm{tr}}\cdot\mathbf{T}_1+\boldsymbol{\mu}^{\mathrm{td}}\cdot\mathbf{g}_0+\sum_{i=1}^{3}\boldsymbol{\mu}_i^{\mathrm{th}}\cdot\mathbf{h}_0^{(i)},\\
\boldsymbol{\Omega}&=\boldsymbol{\omega}_0(\mathbf{R})+\boldsymbol{\mu}^{\mathrm{rt}}\cdot\mathbf{F}_1+\boldsymbol{\mu}^{\mathrm{rr}}\cdot\mathbf{T}_1+\boldsymbol{\mu}^{\mathrm{rd}}\cdot\mathbf{g}_0+\sum_{i=1}^{3}\boldsymbol{\mu}_i^{\mathrm{rh}}\cdot\mathbf{h}_0^{(i)},
\end{aligned} \tag{79}$$

where

$$\boldsymbol{\mu}^{\mathrm{ad}}=\boldsymbol{\mu}^{\mathrm{at}}\cdot\boldsymbol{\zeta}^{\mathrm{td}}+\boldsymbol{\mu}^{\mathrm{ar}}\cdot\boldsymbol{\zeta}^{\mathrm{rd}}, \quad \boldsymbol{\mu}_i^{\mathrm{ah}}=\boldsymbol{\mu}^{\ \mathrm{at}}\cdot\boldsymbol{\zeta}_i^{\mathrm{th}}+\boldsymbol{\mu}^{\mathrm{ar}}\cdot\boldsymbol{\zeta}_i^{\mathrm{rh}}, \tag{80}$$

for a=t, r. Equations (79) give the Stokes velocities of the sphere when subject to external forces, torques, and imposed Poiseuille flow. By equating these velocities to appropriate rates of change of position and orientation of the sphere, we

get the Stokesian dynamics equations[15,23,24] for the motion of an extended spherical particle between hard walls.

The structure of the tensors $\boldsymbol{\zeta}^{ab}$ for a=t, r, d (and hence that of the mobility tensors $\boldsymbol{\mu}^{ab}$) has been analyzed elsewhere[13] for the case of one hard wall into invariant tensors and scalar coefficient functions that depend only on distance from the wall. The two-wall problem has the same two-dimensional translational and rotational symmetry as the one-wall case, so this earlier tensor analysis carries over without change, where now the scalar coefficient functions depend only upon R_z and the aspect ratio W/a. Because we are interested here in Poiseuille flow between the walls, the tensors $\mathbf{g}_0$ and $\mathbf{h}_0^{(i)}$ are not the most general tensors that one would meet in quadratic flow in unbounded fluid. For that reason some of these scalar functions defined earlier for the one-wall case or in unbounded fluid[22] do not contribute and will be omitted from the discussion. The direction normal to the walls is a special direction which we can denote by a unit vector $\hat{\mathbf{n}}$, which, in the coordinate system used here points along the z axis, $\hat{\mathbf{n}}=\mathbf{e}_z$. Using the invariant Cartesian tensors $\delta_{\mu\nu}$ and $\epsilon_{\alpha\mu\nu}$ and the components of $\hat{\mathbf{n}}$, we write the friction tensors in the t, r, and d sectors as

$$\begin{aligned}
\zeta^{tt}_{\alpha\mu}&=\phi^{tt}n_\alpha n_\mu+\psi^{tt}(\delta_{\alpha\mu}-n_\alpha n_\mu),\\
\zeta^{rr}_{\alpha\mu}&=\phi^{rr}n_\alpha n_\mu+\psi^{rr}(\delta_{\alpha\mu}-n_\alpha n_\mu),\\
\zeta^{tr}_{\alpha\mu}&=\psi^{tr}\epsilon_{\alpha\mu\sigma}n_\sigma,\quad \zeta^{rt}_{\alpha\mu}=\psi^{rt}\epsilon_{\alpha\mu\sigma}n_\sigma,\\
\zeta^{td}_{\alpha\mu\nu}&=\psi^{td}\left(\frac{1}{2}\delta_{\alpha\mu}n_\nu+\frac{1}{2}\delta_{\alpha\nu}n_\mu-n_\alpha n_\mu n_\nu\right),\\
\zeta^{rd}_{\alpha\mu\nu}&=\frac{1}{2}\psi^{rd}(n_\sigma\epsilon_{\sigma\alpha\mu}n_\nu+n_\sigma\epsilon_{\sigma\alpha\nu}n_\mu).
\end{aligned}\tag{81}$$

The summation convention applies to repeated subscripts above, and the scalars $\phi^{ab}(R_z)$ and $\psi^{ab}(R_z)$ depend on the position relative to the walls, $-W<R_z<W$. In the h sector, again because of the symmetry of Poiseuille flow, not all possible invariant tensors appear in the decomposition of the $\mathbf{h}_0^{(i)}$. For the two-wall case the effective parts of these tensors are described as

$$\begin{aligned}
\zeta^{th}_{1\alpha\mu}&=\psi^{th}_1(\delta_{\alpha\mu}-n_\alpha n_\mu),\quad \zeta^{rh}_{1\alpha\mu}=\psi^{rh}_1\epsilon_{\alpha\mu\sigma}n_\sigma,\\
\zeta^{th}_{2\alpha\rho\tau\gamma}&=\frac{1}{2}\psi^{th}_2(n_\gamma n_\sigma\epsilon_{\sigma\alpha\mu}\epsilon_{\mu\rho\tau}+n_\sigma\epsilon_{\sigma\alpha\gamma}n_\beta\epsilon_{\beta\rho\tau}),\\
\zeta^{rh}_{2\alpha\rho\tau\gamma}&=\psi^{rh}_2\left(n_\alpha n_\sigma\epsilon_{\sigma\rho\tau}n_\gamma-\frac{1}{2}\delta_{\alpha\gamma}n_\sigma\epsilon_{\sigma\rho\tau}-\frac{1}{2}\epsilon_{\alpha\rho\tau}n_\gamma\right),\\
\zeta^{th}_{3\alpha\rho\tau\gamma}&=\psi^{th}_3\Big(-\frac{1}{15}(\delta_{\alpha\rho}\delta_{\tau\gamma}+\delta_{\alpha\tau}\delta_{\gamma\rho}+\delta_{\alpha\gamma}\delta_{\rho\tau})\\
&\quad+\frac{1}{15}n_\alpha(\delta_{\rho\tau}n_\gamma+\delta_{\tau\gamma}n_\rho+\delta_{\gamma\rho}n_\tau)\\
&\quad+\frac{1}{3}(\delta_{\alpha\rho}n_\tau n_\gamma+\delta_{\alpha\tau}n_\gamma n_\rho+\delta_{\alpha\gamma}n_\rho n_\tau)\\
&\quad-n_\alpha n_\rho n_\tau n_\gamma\Big),
\end{aligned}\tag{82}$$

$$\begin{aligned}
\zeta^{rh}_{3\alpha\rho\tau\gamma}=\frac{1}{3}\psi^{rh}_3\Big[&\epsilon_{\alpha\rho\sigma}n_\sigma\left(n_\tau n_\gamma-\frac{1}{3}\delta_{\tau\gamma}\right)\\
&+\epsilon_{\alpha\tau\sigma}n_\sigma\left(n_\gamma n_\rho-\frac{1}{3}\delta_{\gamma\rho}\right)\\
&+\epsilon_{\alpha\gamma\sigma}n_\sigma\left(n_\rho n_\tau-\frac{1}{3}\delta_{\rho\tau}\right)+\frac{2}{15}(\delta_{\rho\tau}\epsilon_{\alpha\gamma\sigma}n_\sigma\\
&+\delta_{\tau\gamma}\epsilon_{\alpha\rho\sigma}n_\sigma+\delta_{\gamma\rho}\epsilon_{\alpha\tau\sigma}n_\sigma)\Big].
\end{aligned}$$

By comparison of these Cartesian equations with those in the spherical basis, we can express the scalar functions ϕ^{ab} and ψ^{ab} in terms of matrix elements of Z.

To calculate in the spherical basis we start from Eq. (48) for $\ell=1$,

$$f(1m\sigma_1)=\sum_{\ell\sigma_2}Z(1m\sigma_1,\ell m\sigma_2)c(\ell m\sigma_2),\tag{83}$$

where $c(\ell m\sigma)$ has two contributions according to Eq. (41):

$$\begin{aligned}
c(\ell m\sigma)&=c^u(\ell m\sigma)-c^0(\ell m\sigma)\\
&=\langle\mathbf{w}^+_{\ell m\sigma}\delta_a|\mathbf{u}\rangle-\langle\mathbf{w}^+_{\ell m\sigma}\delta_a|\mathbf{v}_0\rangle.
\end{aligned}\tag{84}$$

By explicit calculation using Eqs. (34) and (69), we obtain c^u and c^0 in terms of Cartesian vector and tensor components, which are listed in Appendix C. The only nonzero components are $c^u(1m0)$, $c^u(1m1)$, $c^0(1m0)$, $c^0(1m1)$, $c^0(2m0)$, $c^0(1m2)$, $c^0(2m1)$, and $c^0(3m0)$. The matrix elements $Z(1m\sigma,\ell m\sigma)$ are real, and we have the relation

$$c(\ell -m\sigma)=(-1)^{(m+\sigma)}c^*(\ell m\sigma),\tag{85}$$

so it is sufficient to consider only $m=0$, 1. We have, for these values,

$$\begin{aligned}
f(10\sigma_1)&=\sum_{\sigma_2=0}^{1}Z(10\sigma_1,10\sigma_2)c(10\sigma_2),\\
f(11\sigma_1)&=\sum_{\sigma_2=0}^{1}Z(11\sigma_1,11\sigma_2)c(11\sigma_2)\\
&\quad+Z(11\sigma_1,210)c(210)+Z(11\sigma_1,112)c(112)\\
&\quad+Z(11\sigma_1,211)c(211)+Z(11\sigma_1,310)c(310).
\end{aligned}\tag{86}$$

On inserting the forms of $f(\ell m\sigma)$ and $c(\ell m\sigma)$ from Appendix C and comparing Eqs. (86) with Eqs. (78), we obtain the following expressions for the scalar functions ϕ^{ab} and ψ^{ab}. They are expressed most succinctly in terms of a set of modified matrix elements defined by

$$Z_u(\ell_1m_1\sigma_1,\ell_2m_2\sigma_2)=n_{\ell_1m_1}n_{\ell_2m_2}Z(\ell_1m_1\sigma_1,\ell_2m_2\sigma_2).\tag{87}$$

We find, in terms of these matrix elements,

$$\phi^{tt}=Z_u(100,100), \quad \phi^{rr}=Z_u(101,101),$$

$$\psi^{tt}=\frac{1}{2}Z_u(110,110), \quad \psi^{rr}=\frac{1}{2}Z_u(111,111),$$

$$\psi^{tr}=-\frac{1}{2}Z_u(110,111)=-\frac{1}{2}Z_u(111,110)=-\psi^{rt},$$

$$\psi^{td}=\frac{1}{6}Z_u(110,210), \quad \psi^{rd}=\frac{1}{6}Z_u(111,210), \tag{88}$$

$$\psi_1^{th}=\frac{1}{30}Z_u(110,112), \quad \psi_1^{rh}=\frac{1}{30}Z_u(111,112),$$

$$\psi_2^{th}=\frac{1}{9}Z_u(110,211), \quad \psi_2^{rh}=\frac{1}{9}Z_u(111,211),$$

$$\psi_3^{th}=\frac{1}{12}Z_u(110,310), \quad \psi_3^{rh}=\frac{1}{12}Z_u(111,310).$$

The mobility tensors $\boldsymbol{\mu}^{ab}$ which appear in Eqs. (79) and (80) have precisely the same decomposition in terms of irreducible Cartesian tensors and scalar functions as do the friction tensors $\boldsymbol{\zeta}^{ab}$ as given in Eqs. (81) and (82) with the scalar functions ϕ^{ab} and ψ^{ab} being replaced by α^{ab} and β^{ab}, respectively. These mobility scalars can be expressed also in terms of matrix elements of Z. We observe that for $\sigma=0$, 1 the coefficients $c(1m\sigma)$ contain the components of the rigid body velocities **U** and $\boldsymbol{\Omega}$, so to obtain a mobility equation in the spherical basis we solve Eq. (83) for these four coefficients. To do this we introduce a 2×2 matrix $\mu(1m\sigma_1,1m\sigma_2)$ by the definition

$$\begin{pmatrix} \mu(1m0,1m0) & \mu(1m0,1m1) \\ \mu(1m1,1m0) & \mu(1m1,1m1) \end{pmatrix} = \begin{pmatrix} Z(1m0,1m0) & Z(1m0,1m1) \\ Z(1m1,1m0) & Z(1m1,1m1) \end{pmatrix}^{-1}. \tag{89}$$

We then transform Eq. (83) into

$$\begin{aligned} c(10\sigma_1)&=\sum_{\sigma_2=0}^{1}\mu(10\sigma_1,10\sigma_2)f(10\sigma_2), \\ c(11\sigma_1)&=\sum_{\sigma_2=0}^{1}\mu(11\sigma_1,11\sigma_2)f(11\sigma_2) \\ &\quad-\mu_Z(11\sigma_1,210)c(210)-\mu_Z(11\sigma_1,112)c(112) \\ &\quad-\mu_Z(11\sigma_1,211)c(211)-\mu_Z(11\sigma_1,310)c(310), \end{aligned} \tag{90}$$

where

$$\mu_Z(1m\sigma_1,\ell m\sigma_2)=\sum_{\sigma=0}^{1}\mu(1m\sigma_1,1m\sigma)Z(1m\sigma,\ell m\sigma_2). \tag{91}$$

Now by identifying the mobility equations in the Cartesian (79) and spherical (90) bases, we get expressions for the scalar mobility functions. As for the friction functions, these expressions are most simply stated in terms of a set of modified matrix elements. We define

$$\begin{aligned} \mu_u(1m\sigma_1,1m\sigma_2)&=\frac{1}{n_{1m}^2}\mu(1m\sigma_1,1m\sigma_2), \\ \mu_{Zu}(1m\sigma_1,\ell m\sigma_2)&=\frac{n_{\ell m}}{n_{1m}}\mu_Z(1m\sigma_1,\ell m\sigma_2). \end{aligned} \tag{92}$$

The scalar mobility functions then are

$$\alpha^{tt}=\mu_u(100,100), \quad \alpha^{rr}=\mu_u(101,101),$$

$$\beta^{tt}=2\mu_u(110,110), \quad \beta^{rr}=2\mu_u(111,111),$$

$$\beta^{tr}=-2\mu_u(110,111)=-2\mu_u(111,110)=-\beta^{rt},$$

$$\beta^{td}=\frac{1}{3}\mu_{Zu}(110,210), \quad \beta^{rd}=\frac{1}{3}\mu_{Zu}(111,210), \tag{93}$$

$$\beta_1^{th}=\frac{1}{15}\mu_{Zu}(110,112), \quad \beta_1^{rh}=\frac{1}{15}\mu_{Zu}(111,112),$$

$$\beta_2^{th}=\frac{2}{9}\mu_{Zu}(110,211), \quad \beta_2^{rh}=\frac{2}{9}\mu_{Zu}(111,211),$$

$$\beta_3^{th}=\frac{1}{6}\mu_{Zu}(110,310), \quad \beta_3^{rh}=\frac{1}{6}\mu_{Zu}(111,310).$$

We conclude this section by considering the simplification of the Cartesian equations (78) and (79) which results from applying the general expressions above to the specific Poiseuille flow (69). The tensors $\mathbf{g}_0$ and $\mathbf{h}_0$ arising from the incident flow take a particularly simple form. The only nonvanishing components of these tensors are

$$g_{0yz}=g_{0zy}=-\frac{gR_z}{2\eta}, \quad h_{0yzz}=-\frac{g}{2\eta}. \tag{94}$$

The detailed form of the friction equations (78) is

$$\begin{aligned} F_{1x}&=\psi^{tt}(R_z)U_x+\psi^{tr}(R_z)\Omega_y, \\ F_{1y}&=\psi^{tt}(R_z)\left(U_y-\frac{g}{2\eta}(W^2-R_z^2)\right)-\psi^{tr}(R_z) \\ &\quad\times\left(\Omega_x-\frac{gR_z}{2\eta}\right)+\psi^{td}(R_z)\frac{gR_z}{2\eta}+\psi^{th}(R_z)\frac{g}{2\eta}, \\ F_{1z}&=\phi^{tt}(R_z)U_z, \\ T_{1x}&=\psi^{rt}(R_z)\left(U_y-\frac{g}{2\eta}(W^2-R_z^2)\right) \\ &\quad+\psi^{rr}(R_z)\left(\Omega_x-\frac{gR_z}{2\eta}\right)+\psi^{rd}(R_z)\frac{gR_z}{2\eta} \\ &\quad+\psi^{rh}(R_z)\frac{g}{2\eta}, \\ T_{1y}&=-\psi^{rt}(R_z)U_x+\psi^{rr}(R_z)\Omega_y, \\ T_{1z}&=\phi^{rr}(R_z)\Omega_z. \end{aligned} \tag{95}$$

The Stokes velocities (79) become

$$
\begin{aligned}
U_x &= \beta^{tt}(R_z)F_{1x} + \beta^{tr}(R_z)T_{1y},\\
U_y &= \frac{g}{2\eta}(W^2 - R_z^2) + \beta^{tt}(R_z)F_{1y} - \beta^{tr}(R_z)T_{1x}\\
&\quad - \beta^{td}(R_z)\frac{gR_z}{2\eta} - \beta^{th}(R_z)\frac{g}{2\eta},\\
U_z &= \alpha^{tt}(R_z)F_{1z},\\
\Omega_x &= [1-\beta^{rd}(R_z)]\frac{gR_z}{2\eta} + \beta^{rt}(R_z)F_{1y} + \beta^{rr}(R_z)T_{1x}\\
&\quad - \beta^{rh}(R_z)\frac{g}{2\eta},\\
\Omega_y &= -\beta^{rt}(R_z)F_{1x} + \beta^{rr}(R_z)T_{1y},\\
\Omega_z &= \alpha^{rr}(R_z)T_{1z}.
\end{aligned}
\tag{96}
$$

The functions ϕ^{ab}, ψ^{ab}, α^{ab}, and β^{ab} are functions of R_z, and we have introduced the shorthand

$$
\psi^{ah} = \psi_1^{ah} - \frac{1}{2}\psi_2^{ah} + \frac{4}{15}\psi_3^{ah}, \tag{97}
$$

where a=t, r and β^{ah} is given in terms of the β_i^{ah} by simply changing ψ to β in Eq. (97).

For later comparisons we recall that for a single particle in infinite unbounded fluid we have the Faxén theorem[21]

$$
\mathbf{F}_1 = 6\pi\eta a[\mathbf{U} - \mathbf{v}_0(\mathbf{R})] - \pi\eta a^3\nabla^2\mathbf{v}_0(\mathbf{R}). \tag{98}
$$

By comparing this with the Cartesian equations above, we conclude that in infinite unbounded fluid we have $\psi_{1\infty}^{th} = 2\pi\eta a^3$ and $\beta_{1\infty}^{th} = a^2/3$, while the $\psi_{i\infty}$ and $\beta_{i\infty}$ functions for $i=2$, 3 vanish. The Faxén theorem for the torque $\mathbf{T}_1$ shows that all the corresponding functions in the rh sector vanish in unbounded fluid.

VI. NUMERICAL STUDIES OF FRICTION FUNCTIONS

From the results of Secs. II–V we can obtain the scalar friction and mobility functions which describe the dynamics of a particle between two walls, subject to the flow field (69). We now compare these functions numerically for different values of the aspect ratio W/a. In addition, since we have calculated these functions previously in the t, r, and d sectors for a particle near a single hard wall, we can compare the effect of two walls with that of a single wall and can explore the validity of approximating the two-wall functions by combinations of the single-wall functions.

For numerical comparisons we introduce dimensionless functions $\tilde{\phi}^{ab}$, $\tilde{\psi}^{ab}$, $\tilde{\alpha}^{ab}$, and $\tilde{\beta}^{ab}$ defined as follows:

$$
\begin{aligned}
&\tilde{\phi}^{tt} = \phi^{tt}/6\pi\eta a, \quad \tilde{\psi}^{tt} = \psi^{tt}/6\pi\eta a,\\
&\tilde{\alpha}^{tt} = 6\pi\eta a\,\alpha^{tt}, \quad \tilde{\beta}^{tt} = 6\pi\eta a\,\beta^{tt},\\
&\tilde{\psi}^{tr} = \psi^{tr}/8\pi\eta a^2, \quad \tilde{\beta}^{tr} = 8\pi\eta a^2\beta^{tr},\\
&\tilde{\phi}^{rr} = \phi^{rr}/8\pi\eta a^3, \quad \tilde{\psi}^{rr} = \psi^{rr}/8\pi\eta a^3,\\
&\tilde{\alpha}^{rr} = 8\pi\eta a^3\alpha^{rr}, \quad \tilde{\beta}^{rr} = 8\pi\eta a^3\beta^{rr},\\
&\tilde{\psi}^{td} = \psi^{td}/6\pi\eta a^2, \quad \tilde{\psi}^{rd} = \psi^{rd}/8\pi\eta a^3,\\
&\tilde{\beta}^{td} = \beta^{td}/a, \quad \tilde{\beta}^{rd} = \beta^{rd},\\
&\tilde{\psi}_i^{th} = \psi_i^{th}/2\pi\eta a^3, \quad \tilde{\psi}_i^{rh} = \psi_i^{rh}/2\pi\eta a^4,\\
&\tilde{\beta}_i^{th} = \beta_i^{th}/a^2, \quad \tilde{\beta}_i^{rh} = \beta_i^{rh}/a.
\end{aligned}
\tag{99}
$$

These dimensionless functions of R_z/a are either even or odd. Thus $\tilde{\phi}^{tt}$, $\tilde{\psi}^{tt}$, $\tilde{\phi}^{rr}$, $\tilde{\psi}^{rr}$, $\tilde{\psi}^{rd}$, and $\tilde{\psi}_i^{th}$ are all even functions of R_z/a, while $\tilde{\psi}^{tr}$, $\tilde{\psi}^{td}$, and $\tilde{\psi}_i^{rh}$ are all odd functions of R_z/a. The mobility functions have the same reflection properties on simply changing $\tilde{\phi}^{ab}$ to $\tilde{\alpha}^{ab}$ and $\tilde{\psi}^{ab}$ to $\tilde{\beta}^{ab}$, respectively. Because of the relations (74) and (80), it is clear that the dimensionless mobility functions can be expressed in terms of the dimensionless friction functions so that it is sufficient to calculate the ϕ^{ab} and ψ^{ab} only. We have given these relations elsewhere[13] for the t, r, and d sectors, but for completeness we repeat them here together with the relations that include the h sector:

$$
\begin{aligned}
&\tilde{\alpha}^{tt} = 1/\tilde{\phi}^{tt}, \quad \tilde{\beta}^{tt} = \tilde{\psi}^{rr}/[\tilde{\psi}^{tt}\tilde{\psi}^{rr} - \tfrac{4}{3}(\tilde{\psi}^{tr})^2],\\
&\tilde{\alpha}^{rr} = 1/\tilde{\phi}^{rr}, \quad \tilde{\beta}^{rr} = \tilde{\psi}^{tt}/[\tilde{\psi}^{tt}\tilde{\psi}^{rr} - \tfrac{4}{3}(\tilde{\psi}^{tr})^2],\\
&\tilde{\beta}^{tr} = -\tilde{\psi}^{tr}/[\tfrac{3}{4}\tilde{\psi}^{tt}\tilde{\psi}^{rr} - (\tilde{\psi}^{tr})^2] = -\tilde{\beta}^{rt},\\
&\tilde{\beta}^{td} = \tilde{\beta}^{tt}\tilde{\psi}^{td} - \tilde{\beta}^{tr}\tilde{\psi}^{rd}, \quad \tilde{\beta}^{rd} = \tfrac{3}{4}\tilde{\beta}^{rt}\tilde{\psi}^{td} + \tilde{\beta}^{rr}\tilde{\psi}^{rd},\\
&\tilde{\beta}_i^{th} = \tfrac{1}{3}\tilde{\beta}^{tt}\tilde{\psi}_i^{th} - \frac{1}{4}\tilde{\beta}^{tr}\tilde{\psi}_i^{rh}, \quad \tilde{\beta}_i^{rh} = \tfrac{1}{4}(\tilde{\beta}^{rt}\tilde{\psi}_i^{th} + \tilde{\beta}^{rr}\tilde{\psi}_i^{rh}).
\end{aligned}
\tag{100}
$$

As explained above, the matrix elements of T_1 are calculated by quadrature and are essentially exact. However, to obtain the friction matrix Z from Eq. (49) requires the inversion of an infinite-dimensional matrix ($\ell=1,...,\infty$). Thus in practice we truncate the matrices at order $\ell=\ell_{max}$ and invert the resulting finite-dimensional matrices. By varying ℓ_{max} we can ensure that the approximation has converged for the matrix elements corresponding to the small values of ℓ which occur in Eqs. (88) and (93). For $m=0$, the $\sigma=1$ states do not couple to the $\sigma=0$, 2 states, so the matrices can be partitioned into lower-dimensional matrices for inversion. For $m=1$ there is no such simplification. To obtain an accuracy of four significant figures we have found that if the minimum separation of the particle surface and the wall is no smaller than $0.5a$, then $\ell_{max}=8$ is sufficient with the Fourier integration over q which determines the elements of T_1 as in Eq. (57) cut off at $qa\approx 12$. If this minimum separation is $0.2a$, then ℓ_{max} must increase to 12 and the integration cutoff to $qa\approx 16$. At a still smaller minimum separation of $0.1a$, ℓ_{max} must increase to 16 with the integration cutoff again at $qa\approx 16$. To study the convergence of our scheme we have compared our values of $\tilde{\phi}^{tt}$ with the values of the quantity denoted by $-\lambda$ and calculated by boundary collocation given in Table 5 of Ganatos, Weinbaum, and Pfeffer.[17] To four significant figures our results agree completely with these earlier results. In Table I we illustrate this convergence to five significant figures for the specific case $W/a=2.75$ and $R_z/a=-1.65$. In a second paper[18] the collocation method is applied to motion of the sphere parallel to the two walls. In Table 3 of that reference numerical values are given for the

TABLE I. Numerical values for $\tilde{\phi}^{tt}$ for varying integration cutoffs and different truncations of the matrix dimensionality for $W/a=2.75$ and $R_z/a=-1.65$. These values are to be compared with the value of 11.50 given by boundary collocation (Ref. 17).

ℓ_{max}	$q_{max}=10$	$q_{max}=12$	$q_{max}=14$	$q_{max}=16$	$q_{max}=18$
8	11.2974	11.3051	11.3054	11.3056	11.3056
10	11.4133	11.4479	11.4503	11.4505	11.4505
12	11.4251	11.4775	11.4855	11.4862	11.4862
14	11.4254	11.4809	11.4923	11.4940	11.4942
16	11.4257	11.4810	11.4932	11.4955	11.4959
17	11.4257	11.4811	11.4933	11.4957	11.4961
18	11.4257	11.4811	11.4933	11.4957	11.4962

dimensionless force and torque exerted by the fluid on a sphere held stationary in Poiseuille flow between the two walls. In our notation these quantities denoted as F_x^p and T_y^p can be expressed as

$$F_x^p\left(\frac{R_z}{a}\right)=\left[1-\left(\frac{R_z}{W}\right)^2\right]\tilde{\psi}^{tt}\left(\frac{R_z}{a}\right)-\frac{aR_z}{W^2}\left[\frac{4}{3}\tilde{\psi}^{tr}\left(\frac{R_z}{a}\right)+\tilde{\psi}^{td}\left(\frac{R_z}{a}\right)\right]-\frac{1}{3}\left(\frac{a}{W}\right)^2\tilde{\psi}^{th}\left(\frac{R_z}{a}\right),$$
$$T_y^p\left(\frac{R_z}{a}\right)=\frac{aR_z}{W^2}\left[\tilde{\psi}^{rr}\left(\frac{R_z}{a}\right)-\tilde{\psi}^{rd}\left(\frac{R_z}{a}\right)\right]+\left[1-\left(\frac{R_z}{W}\right)^2\right]\tilde{\psi}^{rt}\left(\frac{R_z}{a}\right)-\frac{1}{4}\left(\frac{a}{W}\right)^2\tilde{\psi}^{rh}\left(\frac{R_z}{a}\right). \quad (101)$$

In Table II we give the values of F_x^p and T_y^p calculated by our technique to five significant figures and compare with the collocation results. The agreement shows the high level of accuracy attainable by both methods. As the particle surface approaches the wall, ℓ_{max} must tend to infinity to reproduce the strong lubrication forces. However, in the region of very close approach to one of the two walls, the lubrication force is dominated by the one-wall result, which we have previously calculated.[13]

To illustrate the two-wall effect we have plotted the dimensionless friction functions $\tilde{\phi}^{tt}$, $\tilde{\psi}^{tt}$, and $\tilde{\psi}^{tr}$ for the cases of channel widths $W/a=5$ and $W/a=2$. Using the fact that the first two of these functions are even functions of R_z/a while the third is odd, we plot only for the range of values $-W/a<R_z/a<0$ corresponding to the particle being between the lower wall and the center of the channel. For comparison we show the corresponding one-wall functions $\tilde{\phi}^{tt}_{1wall}$, $\tilde{\psi}^{tt}_{1wall}$, and $\tilde{\psi}^{tr}_{1wall}$ as well as a superposition approximation in which we superimpose the one-wall functions associated with each wall, taking account of the symmetry of the functions and subtracting out the unbounded fluid result to avoid double counting:

$$\tilde{\phi}^{tt}_{sup}\left(\frac{R_z}{a}\right)=\tilde{\phi}^{tt}_{1wall}\left(\frac{a}{W+R_z}\right)+\tilde{\phi}^{tt}_{1wall}\left(\frac{a}{W-R_z}\right)-1,$$
$$\tilde{\psi}^{tr}_{sup}\left(\frac{R_z}{a}\right)=\tilde{\psi}^{tr}_{1wall}\left(\frac{a}{W+R_z}\right)-\tilde{\psi}^{tr}_{1wall}\left(\frac{a}{W-R_z}\right). \quad (102)$$

Here we express the one-wall functions as functions of the variable a/d where d is the distance from the sphere center to the wall.[13]

TABLE II. Dimensionless force and torque Eq. (101) on a sphere held motionless in a Poiseuille flow between planar walls for a range of aspect ratios W/a.

W/a	F_x^p (Ref. 18)	F_x^p (this work)	T_y^p (Ref. 18)	T_y^p (this work)
2.2	1.347	1.3466	0.2333	0.23331
2.5	1.261	1.2608	0.2058	0.20579
3.0	1.161	1.1612	0.1718	0.17176
4.0	1.044	1.0444	0.1287	0.12868
6.0	0.9364	0.93637	0.08531	0.085306
8.0	0.8858	0.88581	0.06368	0.063679
16.0	0.8147	0.81470	0.03156	0.031557

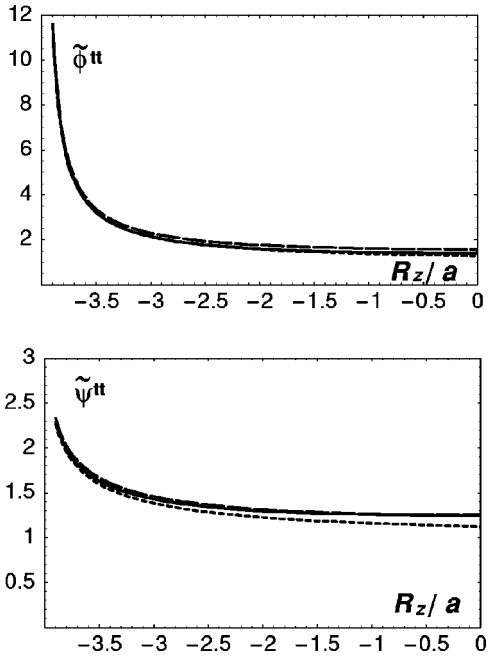

FIG. 2. Dimensionless friction functions $\tilde{\phi}^{tt}$ (upper graphs) and $\tilde{\psi}^{tt}$ (lower graphs) for aspect ratio $W/a=5.0$. The exact result (solid line) is compared with the one-wall result (short-dashed line) and the superposition approximation of Eq. (102) (long-dashed line).

In Fig. 2 we see, for channel width $W/a=5.0$, the friction functions $\tilde{\phi}^{tt}$ and $\tilde{\psi}^{tt}$ corresponding, respectively, to motion normal and parallel to the walls. Note that as the particle approaches the wall the friction functions diverge strongly and their divergence is the same asymptotically as that for the approach to a single wall. In the center of the channel, however, the one-wall result is less than the true result, while the superposition approximation slightly over estimates the correct value. For the narrow channel $W=2a$, we see in Fig. 3 that the deviations from the correct two-wall result are much larger. At the center of the channel the one-wall expression is less than the two-wall result by a considerable margin, while the superposition approximation over estimates $\tilde{\phi}^{tt}$ by more than 15% and underestimates $\tilde{\psi}^{tt}$ by about 4%. In Fig. 3 we see also that the divergence in $\tilde{\psi}^{tt}$ is much weaker (logarithmic) than that in $\tilde{\phi}^{tt}$ (linear).[13] In Fig. 4 we plot the friction function $\tilde{\psi}^{tr}$ and the corresponding mobility

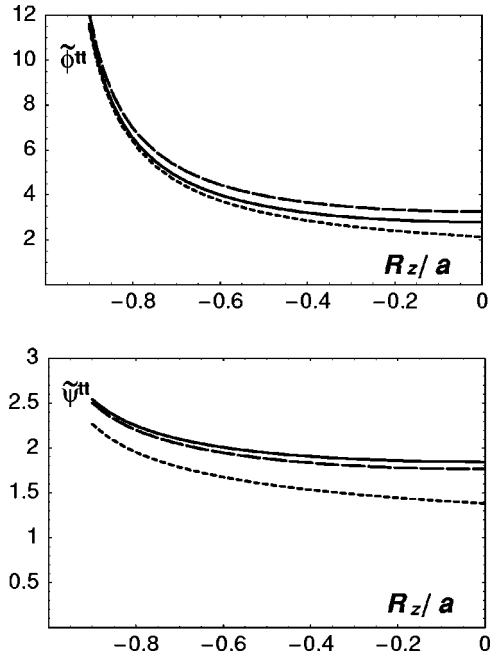

FIG. 3. Dimensionless friction functions $\tilde{\phi}^{tt}$ (upper graphs) and $\tilde{\psi}^{tt}$ (lower graphs) for a narrow channel with aspect ratio $W/a=2.0$. The exact result (solid line) is compared with the one-wall result (short-dashed line) and the superposition approximation of Eq. (102) (long-dashed line).

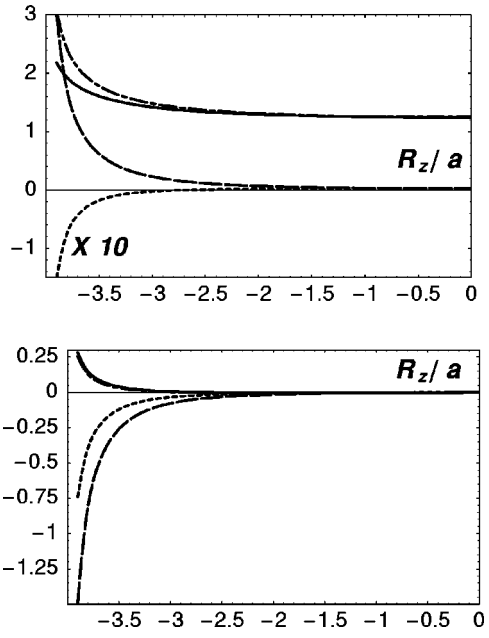

FIG. 5. Dimensionless functions $\tilde{\psi}_i^{th}$, $\tilde{\psi}^{th}$ (upper graphs) and $\tilde{\psi}_i^{rh}$, $\tilde{\psi}^{rh}$ (lower graphs) for aspect ratio $W/a=5.0$. The solid curve gives $\tilde{\psi}_1^{ah}$, the short-dashed curve is $\tilde{\psi}_2^{ah}$, and the long-dashed curve is $\tilde{\psi}_3^{ah}$, while the long-short-dashed curve is $\tilde{\psi}^{ah}$ as in Eq. (97). In the upper graphs $\tilde{\psi}_2^{th}$ has been multiplied by 10 to make it discernible.

$\tilde{\beta}^{tr}$ which describe the translation–rotation coupling. The fascinating behavior here is that for both wide and narrow channels these functions change sign as we cross the channel and neither the one-wall function nor the superposition approximation captures this feature. We show the functions $\tilde{\psi}_i^{ah}$ which give the friction coupling to the Poiseuille flow for the wide channel in Fig. 5 and for the narrow channel in Fig. 6. All numerical calculations have been done using MATHEMATICA 4.0. Representations of all the 13 friction functions as interpolating functions defined in MATHEMATICA are available from the author.

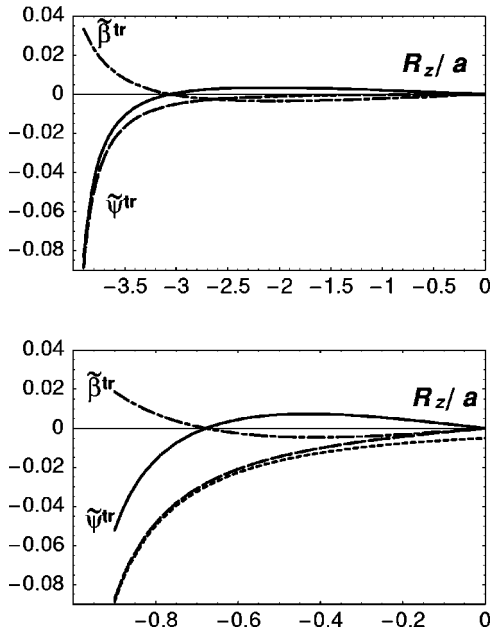

FIG. 4. Dimensionless friction and mobility functions $\tilde{\psi}^{tr}$ and $\tilde{\beta}^{tr}$ for aspect ratio $W/a=5.0$ (upper graphs) and $W/a=2.0$ (lower graphs). The exact friction function (solid line) is compared with the one-wall result (short-dashed line) and the superposition approximation (long-dashed line). For the broader channel the one-wall result overlaps the superposition approximation. The mobility (long-short-dashed line) is calulated from the exact friction functions by use of Eq. (100).

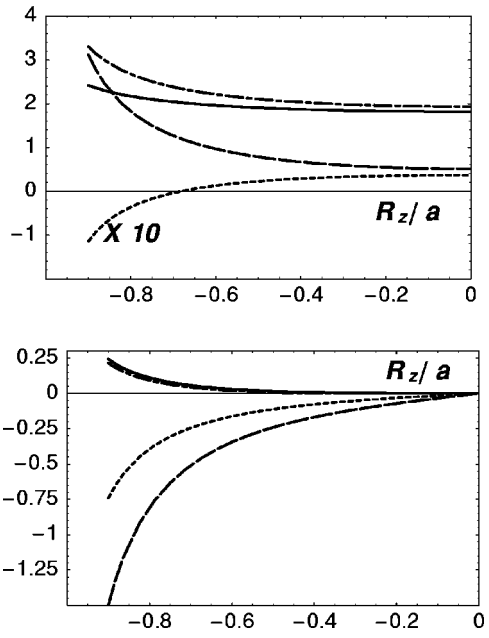

FIG. 6. Dimensionless functions $\tilde{\psi}_i^{th}$, $\tilde{\psi}^{th}$ (upper graphs) and $\tilde{\psi}_i^{rh}$, $\tilde{\psi}^{rh}$ (lower graphs) for a narrow channel with aspect ratio $W/a=2.0$. The solid curve gives $\tilde{\psi}_1^{ah}$, the short-dashed curve is $\tilde{\psi}_2^{ah}$, and the long-dashed curve is $\tilde{\psi}_3^{ah}$, while the long-short-dashed curve is $\tilde{\psi}^{ah}$ as in Eq. (97). In the upper graphs $\tilde{\psi}_2^{th}$ has been multiplied by 10 to make it discernible.

VII. APPLICATION AND CONCLUSIONS

To indicate the effect of the translation–rotation coupling that arises between two walls, we consider finally the motion of a particle carrying a permanent magnetic moment **m** subject to a uniform external magnetic field **H**. We assume the particle to have neutral buoyancy, so there is no external force while the magnetic field produces an external torque $\mathbf{m}\times\mathbf{H}$. In creeping motion this external torque is identical with $\mathbf{T}_1$, the torque which the particle exerts on the fluid. The Stokes velocities (96) simplify somewhat. We define the orientation of the sphere by introducing a body-fixed set of orthogonal axes with coordinate unit vectors $\hat{\mathbf{n}}_1$, $\hat{\mathbf{n}}_2$, and $\hat{\mathbf{n}}_3$. We take $\hat{\mathbf{n}}_3$ to point along the direction of the permanent moment, $\mathbf{m}=m\hat{\mathbf{n}}_3$, and we introduce a fixed unit vector $\hat{\mathbf{h}}$ giving the field direction $\mathbf{H}=H\hat{\mathbf{h}}$. In the absence of external forces there is no motion in the direction normal to the walls, so the particle whose center is at $\mathbf{R}=(R_x,R_y,R_z)$ moves at constant R_z. Using the dimensionless mobilities $\tilde{\beta}^{\mathrm{ab}}(R_z/a)$ of Eqs. (99) and (100) and identifying the Stokes velocities (96) with rates of change of position and orientation, we get the Stokesian dynamics equations for the motion of the sphere in the laboratory frame:

$$
\begin{aligned}
\frac{dR_x}{dt} &= U_x = aD_0^{\mathrm{r}}\Gamma\tilde{\beta}^{\mathrm{tr}}(n_{3z}h_x - n_{3x}h_z),\\
\frac{dR_y}{dt} &= U_y = V_c\left\{\left[1-\left(\frac{R_z}{W}\right)^2\right] - \frac{aR_z}{W^2}\tilde{\beta}^{\mathrm{td}} - \left(\frac{a}{W}\right)^2\tilde{\beta}^{\mathrm{th}}\right\}\\
&\quad - aD_0^{\mathrm{r}}\Gamma\tilde{\beta}^{\mathrm{tr}}(n_{3y}h_z - n_{3z}h_y),\\
\Omega_x &= V_c\left[(1-\tilde{\beta}^{\mathrm{rd}})\frac{R_z}{W^2} - \frac{a}{W^2}\tilde{\beta}^{\mathrm{rh}}\right]\\
&\quad + D_0^{\mathrm{r}}\Gamma\tilde{\beta}^{\mathrm{rr}}(n_{3y}h_z - n_{3z}h_y),\\
\Omega_y &= D_0^{\mathrm{r}}\Gamma\tilde{\beta}^{\mathrm{rr}}(n_{3z}h_x - n_{3x}h_z),\\
\Omega_z &= D_0^{\mathrm{r}}\Gamma\tilde{\alpha}^{\mathrm{rr}}(n_{3x}h_y - n_{3y}h_x),
\end{aligned}
\tag{103}
$$

where the angular velocity $\boldsymbol{\Omega}$ gives the rate of change of orientation through the equations

$$
\frac{d\hat{\mathbf{n}}_i}{dt} = \boldsymbol{\Omega}\times\hat{\mathbf{n}}_i . \tag{104}
$$

In these equations we have introduced the constant velocity $V_c = gW^2/2\eta$, which is the velocity of the Poiseuille flow at the center of the channel, and the quantities $D_0^{\mathrm{r}} = k_BT/8\pi\eta a^3$ and $\Gamma = mH/k_BT$. To form these last two, the thermal energy k_BT involving temperature T and Boltzmann's constant k_B has been introduced on dimensional grounds, although temperature plays no role in Stokesian dynamics where thermal fluctuations and Brownian motion are ignored. However, for application of the theory to mesoscopic particles, only if $\Gamma>1$ can we neglect such fluctuations. When fluctuations are important D_0^{r} is then the rotational diffusion constant[25] which gives a characteristic time for reorientation of such mesoparticles.

To show the influence of translation–rotation coupling, we have integrated the above equations for values of the various parameters corresponding to $a=0.5\,\mu$m, $W=2a$, $T=300$ K, $V_c=2.5\,\mu\mathrm{m\,s}^{-1}$, and η is taken as the viscosity of water. These give $D_0^{\mathrm{r}}=1.32\,\mathrm{s}^{-1}$, and we assume a field strength such that $\Gamma=2$. We take the direction of the external field to be fixed in the x–y plane with direction $\hat{\mathbf{h}}=(1/\sqrt{2},1/\sqrt{2},0)$. The initial condition for position is $R_x(0)=0.0$ and $R_y(0)=0.0$ with two distinct values of the vertical position $R_z/a=-0.85$ and $R_z/a=-0.40$ chosen to correspond to vertical positions where $\tilde{\beta}^{\mathrm{tr}}$ takes positive and negative values, respectively. The initial orientation is described by $\hat{\mathbf{n}}_1=(0,0,1)$, $\hat{\mathbf{n}}_2=(1/\sqrt{2},-1/\sqrt{2},0)$, and $\hat{\mathbf{n}}_3=\hat{\mathbf{h}}$. For each of these two initial conditions the translation–rotation coupling produces motion of the particle in the x direction transverse to the flow direction. We show some features of the solution in Fig. 7. In the upper figure, for initial condition $R_z/a=-0.85$, we show the components of the two orientation vectors $\hat{\mathbf{n}}_1(t)$ and $\hat{\mathbf{n}}_3(t)$. We see that $\hat{\mathbf{n}}_3$, which was initially pointing along the external field direction, rotates to a steady final position in which it is no longer parallel to the field. This reorientation time is about 2 s for the parameters chosen above. From the components of $\hat{\mathbf{n}}_1$ we see that the particle is rotating about this final direction of $\hat{\mathbf{n}}_3$. The lower part of Fig. 7 shows the transverse displacement $R_x(t)$ corresponding to the two values of initial height. Close to the bottom wall this transverse motion is in the direction of negative x, while slightly farther away it is in the positive x direction according to the sign of $\tilde{\beta}^{\mathrm{tr}}$. This extremely interesting phenomenon offers a mechanism for separating suspended dipolar particles dependent on their height in the channel.

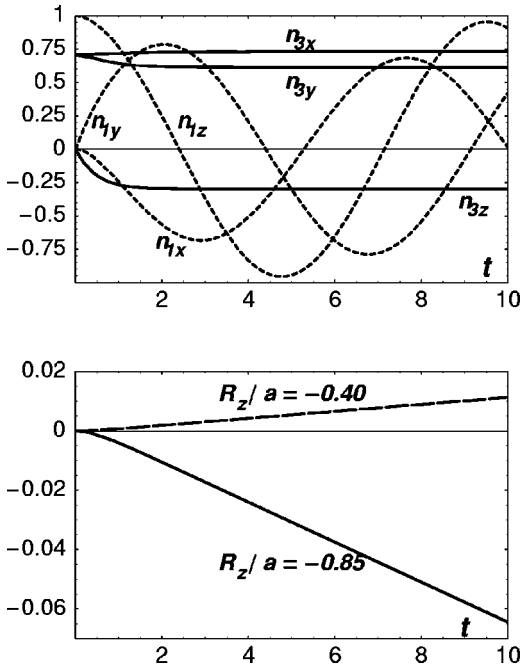

FIG. 7. The upper graphs show Stokesian dynamics results for the orientation of a polar particle in an external magnetic field. The components of the body-fixed unit vectors $\mathbf{n}_1(t)$ (short-dashed line) and $\mathbf{n}_3(t)$ (solid line) are shown as functions of time. In the lower graphs are shown the sideways displacement $R_x(t)/a$ for initial heights $R_z/a=-0.85$ (solid line) and $R_z/a=-0.40$ (dashed line). The motion occurs in a narrow channel with aspect ratio $W/a=2.0$.

We have presented in this work a method of calculating the friction and mobility functions for a single spherical particle in Poiseuille flow between two parallel planar walls. The method depends on having a convenient analytical representation of the Green tensor for the Stokes flow equations in the two-wall geometry. We have shown that the method can be carried through to any desired numerical accuracy. Our results indicate that for aspect ratios such that $W/a>5$ the exact two-wall results are quite well represented by a superposition of single-wall results. For $W/a=5$ the superposition approximation is good to a few percent except that it cannot reproduce the change of sign in the translation–rotation friction and mobility. For a narrow channel $W/a \leqslant 2$, the superposition approximation produces large errors and the exact two-wall results must be used. Already for a single polar particle in an external field the example just above shows interesting dynamical behavior. The strength of our method, however, is that it generalizes to N particles with only minor modifications. The matrix elements needed for N particles are computed with respect to two sphere centers rather than one. These again reduce to quadrature with the integrands containing simple Bessel functions in addition to the terms that appear in Eq. (58) for the one-sphere case. Thus the method presented leads to the possibility of Stokesian dynamics studies of dense clusters of mesoparticles in channel flow between flat walls.

APPENDIX A: SPHERICAL HARMONIC INTEGRALS

The functions $\mathbf{v}^{\pm}_{\ell m\sigma}(\boldsymbol{\epsilon})$ and $\mathbf{w}^{\pm}_{\ell m\sigma}(\boldsymbol{\epsilon})$ are given in full details elsewhere,[15] so here we record only the $\mathbf{w}^{+}_{\ell m\sigma}(\boldsymbol{\epsilon})$ as

$$\mathbf{w}^{+}_{\ell m0}(\boldsymbol{\epsilon})=\frac{1}{\ell(2\ell+1)}\,\epsilon^{-\ell}\left(\mathbf{A}_{\ell m}(\hat{\boldsymbol{\epsilon}})-\frac{2\ell+3}{2}\mathbf{B}_{\ell m}(\hat{\boldsymbol{\epsilon}})\right),$$

$$\mathbf{w}^{+}_{\ell m1}(\boldsymbol{\epsilon})=\frac{i}{\ell(\ell+1)}\,\epsilon^{-\ell-1}\mathbf{C}_{\ell m}(\hat{\boldsymbol{\epsilon}}), \tag{A1}$$

$$\mathbf{w}^{+}_{\ell m2}(\boldsymbol{\epsilon})=\frac{1}{(\ell+1)(2\ell+1)}\,\epsilon^{-\ell-2}\mathbf{B}_{\ell m}(\hat{\boldsymbol{\epsilon}}),$$

where the $\mathbf{A}_{\ell m}(\hat{\boldsymbol{\epsilon}})$, $\mathbf{B}_{\ell m}(\hat{\boldsymbol{\epsilon}})$, and $\mathbf{C}_{\ell m}(\hat{\boldsymbol{\epsilon}})$ are vector spherical harmonics[15,26] dependent on the direction $\hat{\boldsymbol{\epsilon}}$ of the vector $\boldsymbol{\epsilon}$. As mentioned in Sec. IV, we have to integrate the quantities $\mathbf{e}_z\cdot\mathbf{w}^{+}_{\ell m\sigma}(\boldsymbol{\epsilon})$, $\hat{\mathbf{q}}\cdot\mathbf{w}^{+}_{\ell m\sigma}(\boldsymbol{\epsilon})$, and $\hat{\mathbf{q}}\cdot[\mathbf{e}_z\times\mathbf{w}^{+}_{\ell m\sigma}(\boldsymbol{\epsilon})]$ over the direction of $\boldsymbol{\epsilon}$. These quantities may be obtained in terms of the following formulas for the vector spherical harmonics which are derived from their definition[15,26] in terms of scalar harmonics $Y_{\ell m}(\hat{\boldsymbol{\epsilon}})$:

$$n_{\ell m}\mathbf{e}_z\cdot\mathbf{A}_{\ell m}(\hat{\boldsymbol{\epsilon}})=n_{\ell-1m}(\ell+m)Y_{\ell-1m}(\hat{\boldsymbol{\epsilon}}),$$

$$\begin{aligned}n_{\ell m}\hat{\mathbf{q}}\cdot\mathbf{A}_{\ell m}(\hat{\boldsymbol{\epsilon}})=&-\frac{1}{2}[n_{\ell-1m-1}(\ell+m-1)(\ell+m)\\&\times e^{i\phi}Y_{\ell-1m-1}(\hat{\boldsymbol{\epsilon}})-n_{\ell-1m+1}\\&\times e^{-i\phi}Y_{\ell-1m+1}(\hat{\boldsymbol{\epsilon}})],\end{aligned} \tag{A2}$$

$$n_{\ell m}\hat{\mathbf{q}}\cdot[\mathbf{e}_z\times\mathbf{A}_{\ell m}(\hat{\boldsymbol{\epsilon}})]=\frac{i}{2}[n_{\ell-1m-1}(\ell+m-1)(\ell+m)\times e^{i\phi}Y_{\ell-1m-1}(\hat{\boldsymbol{\epsilon}})+n_{\ell-1m+1}\times e^{-i\phi}Y_{\ell-1m+1}(\hat{\boldsymbol{\epsilon}})],$$

$$n_{\ell m}\mathbf{e}_z\cdot\mathbf{B}_{\ell m}(\hat{\boldsymbol{\epsilon}})=-n_{\ell+1m}(\ell-m+1)Y_{\ell+1m}(\hat{\boldsymbol{\epsilon}}),$$

$$\begin{aligned}n_{\ell m}\hat{\mathbf{q}}\cdot\mathbf{B}_{\ell m}(\hat{\boldsymbol{\epsilon}})=&-\frac{1}{2}[n_{\ell+1m-1}(\ell-m+1)(\ell-m+2)\\&\times e^{i\phi}Y_{\ell+1m-1}(\hat{\boldsymbol{\epsilon}})-n_{\ell+1m+1}\\&\times e^{-i\phi}Y_{\ell+1m+1}(\hat{\boldsymbol{\epsilon}})],\end{aligned} \tag{A3}$$

$$n_{\ell m}\hat{\mathbf{q}}\cdot[\mathbf{e}_z\times\mathbf{B}_{\ell m}(\hat{\boldsymbol{\epsilon}})]=\frac{i}{2}[n_{\ell+1m-1}(\ell-m+1)\times(\ell-m+2)e^{i\phi}Y_{\ell+1m-1}(\hat{\boldsymbol{\epsilon}})+n_{\ell+1m+1}e^{-i\phi}Y_{\ell+1m+1}(\hat{\boldsymbol{\epsilon}})],$$

$$\mathbf{e}_z\cdot\mathbf{C}_{\ell m}(\hat{\boldsymbol{\epsilon}})=-imY_{\ell m}(\hat{\boldsymbol{\epsilon}}),$$

$$\begin{aligned}n_{\ell m}\hat{\mathbf{q}}\cdot\mathbf{C}_{\ell m}(\hat{\boldsymbol{\epsilon}})=&-\frac{i}{2}[n_{\ell m-1}(\ell+m)(\ell-m+1)\\&\times e^{i\phi}Y_{\ell m-1}(\hat{\boldsymbol{\epsilon}})\\&+n_{\ell m+1}e^{-i\phi}Y_{\ell m+1}(\hat{\boldsymbol{\epsilon}})],\end{aligned} \tag{A4}$$

$$\begin{aligned}n_{\ell m}\hat{\mathbf{q}}\cdot[\mathbf{e}_z\times\mathbf{C}_{\ell m}(\hat{\boldsymbol{\epsilon}})]=&-\frac{1}{2}[n_{\ell m-1}(\ell+m)(\ell-m+1)\\&\times e^{i\phi}Y_{\ell m-1}(\hat{\boldsymbol{\epsilon}})-n_{\ell m+1}e^{-i\phi}\\&\times Y_{\ell m+1}(\hat{\boldsymbol{\epsilon}})].\end{aligned}$$

In these formulas ϕ is the polar angle of the two-dimensional wave vector $\mathbf{q}$, $q_x=q\cos\phi$ and $q_y=q\sin\phi$.

The definition and identities (A1)–(A4) lead to the quantities $K_{\ell m}(\mathbf{q})$ and $L_{\ell m}(\mathbf{q})$ introduced in Eqs. (60) and (61). These functions are defined in terms of integrals whose integrands involve a spherical harmonic $Y_{\ell m}(\hat{\boldsymbol{\epsilon}})$ multiplied by exponential functions that depend on the components of the vector $\boldsymbol{\epsilon}$ which has fixed length $\epsilon=|\boldsymbol{\epsilon}|=a$ where a is the particle radius. We sketch here the derivation of the analytical results (62)–(65) in Sec. IV. We begin by looking at the integral

$$K_{\ell m}(x,y,z)=a\int d\Omega\, Y_{\ell m}(\hat{\boldsymbol{\epsilon}})e^{-i\mathbf{r}\cdot\boldsymbol{\epsilon}}, \tag{A5}$$

where $\mathbf{r}=(x,y,z)$ is a fixed vector, $Y_{\ell m}(\hat{\boldsymbol{\epsilon}})$ is the spherical harmonic $Y_{\ell m}(\theta_\epsilon,\phi_\epsilon)$ depending on the direction of $\boldsymbol{\epsilon}$, and $d\Omega$ is the solid angle $\sin\theta_\epsilon d\theta_\epsilon d\phi_\epsilon$. This integral is commonly met in quantum-mechanical scattering theory where we have the identity[26]

$$e^{-i\mathbf{r}\cdot\boldsymbol{\epsilon}}=4\pi\sum_{n=0}^{\infty}e^{-in\pi/2}j_n(r\epsilon)\sum_{m=-n}^{m=n}Y_{nm}(\hat{\mathbf{r}})Y^{*}_{nm}(\hat{\boldsymbol{\epsilon}}), \tag{A6}$$

with $j_n(r\epsilon)$ a spherical Bessel function.[27] Combining these two equations and using the orthogonality of the spherical harmonics gives

$$K_{\ell m}(x,y,z)=4\pi a e^{-i\ell\pi/2} j_\ell(r\epsilon) Y_{\ell m}(\hat{\mathbf{r}})$$

$$=4\pi a e^{-i\ell\pi/2}\frac{j_\ell(r\epsilon)}{r^\ell}\mathcal{Y}_{\ell m}(\mathbf{r}), \tag{A7}$$

where we have introduced the solid harmonic $\mathcal{Y}_{\ell m}(\mathbf{r})=r^\ell Y_{\ell m}(\hat{\mathbf{r}})$ as defined by Edmonds.[26] Although the derivation above was carried out for real values of $\mathbf{r}$ and $\boldsymbol{\epsilon}$, the result (A7) remains valid for complex values of the vector components of $\mathbf{r}$. Thus we analytically continue the components of $\mathbf{r}$ to $x=q_x$, $y=q_y$, and $z=-is$, giving

$$K_{\ell m}(q_x,q_y,-is)=a\int d\Omega\, Y_{\ell m}(\hat{\boldsymbol{\epsilon}})e^{-i\mathbf{q}\cdot\boldsymbol{\Delta}}e^{-s\epsilon_z}$$

$$=4\pi a e^{-i\ell\pi/2}\frac{j_\ell(r\epsilon)}{r^\ell}\mathcal{Y}_{\ell m}(q_x,q_y,-is), \tag{A8}$$

where $\boldsymbol{\Delta}=(\epsilon_x,\epsilon_y)$ is a two-dimensional vector as in Sec. IV and $r=\sqrt{q^2-s^2}$. Finally, take the limits $s\to q=\sqrt{q_x^2+q_y^2}$, which is equivalent to the limit $r\to 0$. Using the behavior of the spherical Bessel function in this limit gives the result (62).

We next need an explicit formula for the solid harmonic $\mathcal{Y}_{\ell m}(q_x,q_y,-is)$ evaluated at complex argument. To obtain this we introduce an auxiliary family of harmonic polynomials $G_{\ell m}(\mathbf{r})=G_{\ell m}(x,y,z)$ defined by the generating function

$$G(\mathbf{r},t)=[(x-iy)+2zt-(x+iy)t^2]^\ell$$

$$=t^\ell\sum_{m=-\ell}^{m=\ell}G_{\ell m}(\mathbf{r})t^m. \tag{A9}$$

Note that these polynomials are defined slightly differently from the related polynomials introduced by Edmonds.[26] We first show that the $G_{\ell m}(\mathbf{r})$ are proportional to the $\mathcal{Y}_{\ell m}(\mathbf{r})$. We observe from the generating function definition that

$$G_{\ell\ell}(\mathbf{r})=(-1)^\ell(x+iy)^\ell=(-1)^\ell r^\ell(\sin\theta)^\ell e^{i\ell\phi}, \tag{A10}$$

where θ and ϕ are the spherical polar angles of $\mathbf{r}$. From Edmonds, we have

$$\mathcal{Y}_{\ell\ell}(\mathbf{r})=\frac{(-1)^\ell r^\ell}{n_{\ell\ell}}P_\ell^\ell(\cos\theta)e^{i\ell\phi}$$

$$=\frac{(-1)^\ell r^\ell(2\ell)!}{n_{\ell\ell}2^\ell\ell!}(\sin\theta)^\ell e^{i\ell\phi}, \tag{A11}$$

where $n_{\ell\ell}$ is the normalization coefficient introduced in Eq. (64) for $m=\ell$ and we have used the explicit form of the associated Legendre polynomial $P_\ell^\ell(\cos\theta)$. It is clear, for $m=\ell$, that $G_{\ell\ell}$ is proportional to $\mathcal{Y}_{\ell\ell}$:

$$G_{\ell\ell}(\mathbf{r})=\frac{2^\ell\ell!}{(2\ell)!}n_{\ell\ell}\mathcal{Y}_{\ell\ell}(\mathbf{r}). \tag{A12}$$

The next step is to use the quantum-mechanical lowering operator $\hat{L}_-$ on both sides of this equation to shift the m values.[26] Putting Planck's constant equal to 1, this operator has the form $\hat{L}_-=\hat{L}_x-i\hat{L}_y=(x-iy)\partial/\partial z-z(\partial/\partial x-i\partial/\partial y)$, and from the theory of angular momentum we have[26]

$$\hat{L}_-\mathcal{Y}_{\ell m}(\mathbf{r})=\sqrt{(\ell+m)(\ell-m+1)}\,\mathcal{Y}_{\ell m-1}(\mathbf{r}), \tag{A13}$$

while from the generating function definition one can easily show that

$$\hat{L}_-G_{\ell m}(\mathbf{r})=(\ell-m+1)G_{\ell m-1}(\mathbf{r}). \tag{A14}$$

Applying $\hat{L}_-$ repeatedly to both sides of Eq. (A12) gives

$$\mathcal{Y}_{\ell m}(\mathbf{r})=\frac{(\ell+m)!}{n_{\ell m}2^\ell\ell!}G_{\ell m}(\mathbf{r}). \tag{A15}$$

We evaluate $G_{\ell m}(q_x,q_y,-is)$ by observing that $G_{\ell m}$ is the residue of $G(\mathbf{r},t)/t^{\ell+m+1}$ at $t=0$. We express this residue by a Cauchy integral on a unit circle in the t plane encircling $t=0$. For $\mathbf{r}=(q_x,q_y,-is)$ it is easy to reduce the contour integral to the form

$$G_{\ell m}(q_x,q_y,-is)$$

$$=\frac{(-2is)^\ell}{2\pi}e^{im\phi}\int_0^{2\pi}(1+\sin\alpha)^\ell e^{-im\alpha}d\alpha. \tag{A16}$$

This integral reduces to a standard integral[28]

$$\int_0^{2\pi}(1+\sin\alpha)^\ell e^{-im\alpha}d\alpha$$

$$=2^{\ell+2}e^{-im\pi/2}\int_0^{\pi/2}(\cos\beta)^{2\ell}\cos 2m\beta d\beta. \tag{A17}$$

Putting together Eqs. (A8) and (A15)–(A17) gives the results (62) and (63) in Sec. IV. The additional integrals denoted as $L_{\ell m}^{\pm}(\mathbf{q})$ in Sec. IV have an extra factor of ϵ_z in the integrand as compared with $K_{\ell m}^{\pm}(\mathbf{q})$. Such integrals are evaluated by differentiating Eq. (A8) with respect to s before taking the limit $s\to q$.

APPENDIX B: TABULATION OF $\mathcal{I}_{\ell m\sigma}$, $\mathcal{J}_{\ell m\sigma}$, AND $\mathcal{H}_{\ell m\sigma}$

The integrals evaluated in Appendix A can be used in combination to obtain the quantities $I_{\ell m\sigma}^{(k)}$, $J_{\ell m\sigma}^{(k)}$, and $H_{\ell m\sigma}^{(k)}$ for $k=1,\ldots,4$. We simply tabulate the results below. The most complicated expressions correspond to $\sigma=0$, and we give these first. Remembering that $\mathbf{q}=(q_x,q_y)=(q\cos\phi,q\sin\phi)$ and introducing the coefficient

$$C_{\ell m0}=\frac{n_{\ell m}a^{-\ell+1}e^{-i\ell\pi/2}}{\ell(\ell+m)!}, \tag{B1}$$

we find

$$I_{\ell m0}^{(1)}(\mathbf{q})=iC_{\ell m0}\sin(\ell+m)\frac{\pi}{2}\left(\frac{(\ell^2-m^2)}{2\ell-1}(qa)^{\ell-1}\right.$$

$$\left.+\frac{1}{2}(qa)^{\ell+1}\right)e^{im\phi}, \tag{B2}$$

$$I^{(4)}_{\ell m0}(\mathbf{q}) = iC_{\ell m0}\sin(\ell+m)\frac{\pi}{2} \times\left[\frac{(\ell^2-m^2)}{2\ell-1}\left(\frac{(\ell-1)^2-m^2}{2\ell-3}(qa)^{\ell-1} + \frac{1}{2\ell+1}(qa)^{\ell+1}\right) + \frac{1}{2}\left(\frac{(\ell+1)^2-m^2}{2\ell+1}(qa)^{\ell+1} + \frac{1}{2\ell+5}(qa)^{\ell+3}\right)\right]e^{im\phi}.$$

The terms $I^{(2)}_{\ell m0}(\mathbf{q})$ and $I^{(3)}_{\ell m0}(\mathbf{q})$ arise, respectively, from $I^{(1)}_{\ell m0}(\mathbf{q})$ and $I^{(4)}_{\ell m0}(\mathbf{q})$ by replacing $i\sin(\ell+m)\pi/2$ with $\cos(\ell+m)\pi/2$. Next, we have

$$J^{(1)}_{\ell m0}(\mathbf{q}) = \frac{i}{2}C_{\ell m0}\cos(\ell+m)\frac{\pi}{2} \times\left(\frac{2[\ell(\ell-1)+m^2]}{2\ell-1}(qa)^{\ell-1} - (qa)^{\ell+1}\right)e^{im\phi}, \tag{B3}$$

$$J^{(4)}_{\ell m0}(\mathbf{q}) = \frac{i}{2}C_{\ell m0}\cos(\ell+m)\frac{\pi}{2} \times\left[\frac{2(\ell^2-m^2)[(\ell-2)(\ell-1)+m^2]}{(2\ell-1)(2\ell-3)}(qa)^{\ell-1} + \frac{2[\ell(\ell-1)+m^2]}{(2\ell-1)(2\ell+1)}(qa)^{\ell+1} - \frac{(\ell+1)^2-m^2-1}{2\ell+1}(qa)^{\ell+1} - \frac{1}{2\ell+5}(qa)^{\ell+3}\right]e^{im\phi},$$

and $J^{(2)}_{\ell m0}(\mathbf{q})$ and $J^{(3)}_{\ell m0}(\mathbf{q})$ arise, respectively, from $J^{(1)}_{\ell m0}(\mathbf{q})$ and $J^{(4)}_{\ell m0}(\mathbf{q})$ by replacing $i\cos(\ell+m)\pi/2$ with $-\sin(\ell+m)\pi/2$. For the $H^{(k)}_{\ell m0}$ we have

$$H^{(2)}_{\ell m0}(\mathbf{q}) = imC_{\ell m0}\sin(\ell+m)\frac{\pi}{2}(qa)^{\ell-1}e^{im\phi}, \tag{B4}$$

$$H^{(3)}_{\ell m0}(\mathbf{q}) = imC_{\ell m0}\sin(\ell+m)\frac{\pi}{2}\frac{\ell^2-m^2}{2\ell-1}(qa)^{\ell-1}e^{im\phi},$$

and $H^{(1)}_{\ell m0}$ and $H^{(4)}_{\ell m0}$ arise, respectively, from $H^{(2)}_{\ell m0}$ and $H^{(3)}_{\ell m0}$ by replacing $i\sin(\ell+m)\pi/2$ with $\cos(\ell+m)\pi/2$.

For $\sigma=1$ we define

$$C_{\ell m1} = \frac{n_{\ell m}a^{-\ell}e^{-i\ell\pi/2}}{\ell(\ell+1)(\ell+m)!}, \tag{B5}$$

and then find

$$I^{(2)}_{\ell m1}(\mathbf{q}) = imC_{\ell m1}\sin(\ell+m)\frac{\pi}{2}(qa)^{\ell}e^{im\phi},$$

$$I^{(3)}_{\ell m1}(\mathbf{q}) = imC_{\ell m1}\sin(\ell+m)\frac{\pi}{2}\left(\frac{(\ell^2-m^2)}{2\ell-1}(qa)^{\ell} + \frac{1}{2\ell+3}(qa)^{\ell+2}\right)e^{im\phi}, \tag{B6}$$

where the replacement of $i\sin(\ell+m)\pi/2$ by $\cos(\ell+m)\pi/2$ in $I^{(2)}_{\ell m1}$ and $I^{(3)}_{\ell m1}$ gives $I^{(1)}_{\ell m1}$ and $I^{(4)}_{\ell m1}$, respectively. For the $J^{(k)}_{\ell m1}$ we have

$$J^{(2)}_{\ell m1}(\mathbf{q}) = -imC_{\ell m1}\cos(\ell+m)\frac{\pi}{2}(qa)^{\ell}e^{im\phi},$$

$$J^{(3)}_{\ell m1}(\mathbf{q}) = -imC_{\ell m1}\cos(\ell+m)\frac{\pi}{2} \times\left(\frac{(\ell+1)^2-m^2-2}{2\ell-1}(qa)^{\ell} + \frac{1}{2\ell+3}(qa)^{\ell+2}\right)e^{im\phi}, \tag{B7}$$

and by replacing $-i\cos(\ell+m)\pi/2$ by $\sin(\ell+m)\pi/2$ we get $J^{(1)}_{\ell m1}$ and $J^{(4)}_{\ell m1}$, respectively. For the $H^{(k)}_{\ell m1}$ we have

$$H^{(1)}_{\ell m1}(\mathbf{q}) = -i\ell C_{\ell m1}\sin(\ell+m)\frac{\pi}{2}(qa)^{\ell}e^{im\phi},$$

$$H^{(4)}_{\ell m1}(\mathbf{q}) = -iC_{\ell m1}\sin(\ell+m)\frac{\pi}{2} \times\left(\frac{\ell(\ell^2-1)-m^2(\ell-2)}{2\ell-1}(qa)^{\ell} + \frac{\ell}{2\ell+3}(qa)^{\ell+2}\right)e^{im\phi}, \tag{B8}$$

and the replacement of $i\sin(\ell+m)\pi/2$ by $\cos(\ell+m)\pi/2$ gives, respectively, $H^{(2)}_{\ell m1}$ and $H^{(3)}_{\ell m1}$.

Finally, for $\sigma=2$ we define

$$C_{\ell m2} = \frac{n_{\ell m}a^{-\ell-1}e^{-i\ell\pi/2}}{(\ell+1)(2\ell+3)(\ell+m)!} \tag{B9}$$

and find

$$I^{(1)}_{\ell m2}(\mathbf{q}) = -iC_{\ell m2}\sin(\ell+m)\frac{\pi}{2}(qa)^{\ell+1}e^{im\phi},$$

$$I^{(4)}_{\ell m2}(\mathbf{q}) = -iC_{\ell m2}\sin(\ell+m)\frac{\pi}{2}\left(\frac{(\ell+1)^2-m^2}{2\ell+1}(qa)^{\ell+1} + \frac{1}{2\ell+5}(qa)^{\ell+3}\right)e^{im\phi}, \tag{B10}$$

where the replacement of $i\sin(\ell+m)\pi/2$ by $\cos(\ell+m)\pi/2$ gives $I^{(2)}_{\ell m2}$ and $I^{(3)}_{\ell m2}$, respectively. Next, we have

$$J^{(1)}_{\ell m2}(\mathbf{q}) = iC_{\ell m2}\cos(\ell+m)\frac{\pi}{2}(qa)^{\ell+1}e^{im\phi},$$

$$J^{(4)}_{\ell m2}(\mathbf{q}) = iC_{\ell m2}\cos(\ell+m)\frac{\pi}{2} \times\left(\frac{(\ell+1)^2-m^2-1}{2\ell+1}(qa)^{\ell+1} + \frac{1}{2\ell+5}(qa)^{\ell+3}\right)e^{im\phi}, \tag{B11}$$

for which the replacement of $i\cos(\ell+m)\pi/2$ by $-\sin(\ell+m)\pi/2$ gives $J^{(2)}_{\ell m2}$ and $J^{(3)}_{\ell m2}$, respectively. Last, we find

$$H^{(1)}_{\ell m2}(\mathbf{q}) = 0, \quad H^{(2)}_{\ell m2}(\mathbf{q}) = 0, \tag{B12}$$

and

$$H^{(3)}_{\ell m2}(\mathbf{q}) = \frac{2}{2\ell+1}imC_{\ell m2}\sin(\ell+m)\frac{\pi}{2}(qa)^{\ell+1}e^{im\phi},$$

$$H^{(4)}_{\ell m2}(\mathbf{q}) = \frac{2}{2\ell+1}mC_{\ell m2}\cos(\ell+m)\frac{\pi}{2}(qa)^{\ell+1}e^{im\phi}. \tag{B13}$$

APPENDIX C: SPHERICAL COMPONENTS OF FORCE AND FLOW

We collect here the expressions for the $c(\ell m\sigma)$ and $f(\ell m\sigma)$ used in Sec. V to relate the friction and mobility functions in the Cartesian and spherical bases. Because of the symmetry of Z, we need only the $m=0$, 1 components. Just as with the matrix elements in Sec. V, we can simplify the expressions by defining

$$c(\ell m\sigma) = n_{\ell m}c_u(\ell m\sigma), \quad f(\ell m\sigma) = \frac{1}{n_{\ell m}}f_u(\ell m\sigma). \tag{C1}$$

We then find

$$c_u(100) = U_z - v_{0z}(\mathbf{R}), \quad c_u(101) = -i[\Omega_z - \omega_{0z}(\mathbf{R})],$$

$$c_u(110) = \frac{1}{2}\{-[U_x - v_{0x}(\mathbf{R})] + i[U_y - v_{0y}(\mathbf{R})]\},$$

$$c_u(111) = \frac{1}{2}\{[\Omega_y - \omega_{0y}(\mathbf{R})] + i[\Omega_x - \omega_{0x}(\mathbf{R})]\},$$

$$c_u(210) = \frac{1}{6}(g_{0zx} - ig_{0zy}),$$

$$c_u(112) = -\frac{1}{30}(h^{(1)}_{0x} - ih^{(1)}_{0y}),$$

$$c_u(211) = \frac{1}{18}[-(h_{0xyy} - h_{0yxy} - h_{0xzz} + h_{0zxz}) + i(-h_{0xyx} + h_{0yxx} - h_{0yzz} + h_{0zyz})],$$

$$c_u(310) = -\frac{1}{180}\{[-(3h_{0xxx} + h_{0xyy} - 4h_{0xzz}) - (h_{0yxy} + h_{0yyx}) + 4(h_{0zzx} + h_{0zxz})] + i[(3h_{0yyy} + h_{0yxx} - 4h_{0yzz}) + (h_{0xyx} + h_{0xxy}) - 4(h_{0zzy} + h_{0zyz})]\}. \tag{C2}$$

As noted in Sec. V, in Eqs. (94), for the particular flow assumed in Eqs. (69), most of the elements $h_{0\rho\tau\gamma}$ vanish. For the force multipoles we have

$$f_u(100) = F_{1z}, \quad f_u(101) = -iT_{1z},$$

$$f_u(110) = -F_{1x} + iF_{1y}, \quad f_u(111) = T_{1y} + iT_{1x}. \tag{C3}$$

[1] P. N. Pusey, in *Liquids, Freezing and Glass Transition*, edited by J. P. Hansen, D. Levesque, and J. Zinn-Justin (North-Holland, Amsterdam, 1991).
[2] R. B. Jones and P. N. Pusey, Annu. Rev. Phys. Chem. **42**, 137 (1991).
[3] B. Cichocki, M. L. Ekiel-Jeżewska, and E. Wajnryb, J. Chem. Phys. **111**, 3265 (1999).
[4] A. J. C. Ladd, J. Chem. Phys. **90**, 1149 (1989).
[5] R. B. Jones and R. Kutteh, J. Chem. Phys. **112**, 11080 (2000).
[6] K. H. Lan, N. Ostrowsky, and D. Sornette, Phys. Rev. Lett. **57**, 17 (1986).
[7] L. Lobry and N. Ostrowsky, Phys. Rev. B **53**, 12050 (1996).
[8] Y. Grasselli and L. Lobry, Phys. Fluids **9**, 3929 (1997).
[9] E. R. Dufresne, T. M. Squires, M. P. Brenner, and D. G. Grier, Phys. Rev. Lett. **85**, 3317 (2000).
[10] A. T. Skjeltorp, J. Appl. Phys. **57**, 3285 (1985).
[11] K. Zahn and G. Maret, Phys. Rev. Lett. **85**, 3656 (2000).
[12] P. T. Korda, M. B. Taylor, and D. G. Grier, Phys. Rev. Lett. **89**, 128301 (2002).
[13] B. Cichocki and R. B. Jones, Physica A **258**, 273 (1998).
[14] R. Schmitz and B. U. Felderhof, Physica A **113**, 90 (1982).
[15] B. Cichocki, R. B. Jones, R. Kutteh, and E. Wajnryb, J. Chem. Phys. **112**, 2548 (2000).
[16] B. P. Ho and L. G. Leal, J. Fluid Mech. **65**, 365 (1974).
[17] P. Ganatos, S. Weinbaum, and R. Pfeffer, J. Fluid Mech. **99**, 739 (1980).
[18] P. Ganatos, R. Pfeffer, and S. Weinbaum, J. Fluid Mech. **99**, 755 (1980).
[19] S. Bhattacharya and J. Blawzdziewicz, J. Math. Phys. **43**, 5720 (2002).
[20] N. Liron and S. Mochon, J. Eng. Math. **10**, 287 (1976).
[21] J. Happel and H. Brenner, *Low Reynolds Number Hydrodynamics* (Noordhoff, Leiden, 1973).
[22] B. Cichocki, B. U. Felderhof, and R. Schmitz, PhysicoChem. Hydrodyn. **10**, 383 (1988).
[23] L. Durlofsky, J. F. Brady, and G. Bossis, J. Fluid Mech. **180**, 21 (1987).
[24] J. F. Brady and G. Bossis, Annu. Rev. Fluid Mech. **20**, 111 (1988).
[25] R. B. Jones, Physica A **150**, 339 (1988).
[26] A. R. Edmonds, *Angular Momentum in Quantum Mechanics* (Princeton University Press, Princeton, 1957).
[27] *Handbook of Mathematical Functions*, edited by Milton Abramowitz and Irene A. Stegun (Dover, New York, 1965).
[28] I. S. Gradshteyn and I. M. Ryzhik, *Table of Integrals, Series and Products* (Academic, New York, 1980), integral 3.631(9).